

UNIVERSIDADE ESTADUAL DE CAMPINAS

INSTITUTO DE BIOLOGIA

JANE CRISTINA DE SOUZA

“SECREÇÃO E AÇÃO DA INSULINA EM CAMUNDONGOS

KNOCKOUT PARA O RECEPTOR DE LDL (LDLR^{-/-})

ALIMENTADOS COM DIETA PADRÃO OU HIPERLIPÍDICA”

Este exemplar corresponde à redação final
da tese defendida pelo(a) candidato (a)

Jane Cristina de Souza
Boschiero

e aprovada pela Comissão Julgadora.

Tese apresentada ao Instituto de Biologia para obtenção do Título de Doutor em Biologia Funcional e Molecular, na área de Fisiologia.

Orientador: Prof. Dr. Antonio Carlos Boschiero

Co-Orientadora: Profa. Dra. Helena Coutinho Franco de Oliveira

Campinas, 2012

FICHA CATALOGRÁFICA ELABORADA POR
ROBERTA CRISTINA DAL'EVEDOVE TARTAROTTI - CRB8/7430
BIBLIOTECA DO INSTITUTO DE BIOLOGIA - UNICAMP

Souza, Jane Cristina de, 1981-
So89s Secreção e ação da insulina em camundongos knockout para o receptor de LDL (LDLR -/-) alimentados com dieta padrão ou hiperlipídica / Jane Cristina de Souza. – Campinas, SP: [s.n.], 2012.

Orientador: Antonio Carlos Boschiero.
Coorientador: Helena Coutinho Franco de Oliveira.
Tese (doutorado) – Universidade Estadual de Campinas, Instituto de Biologia.

1. Insulina - Secreção. 2. Colesterol. 3. Movimentação de cálcio. 4. Dieta hiperlipídica. 5. Resistência à insulina. 6. Receptores LDL. I. Boschiero, Antonio Carlos, 1943-. II. Oliveira, Helena Coutinho Franco de, 1958-. III. Universidade Estadual de Campinas. Instituto de Biologia. IV. Título.

Informações para Biblioteca Digital

Titulo em Inglês: Secretion and action of the insulin on LDL receptor knockout mice (LDLR -/-) fed with chow or hyperlipidic diet

Palavras-chave em Inglês:

Insulin - Secretion

Cholesterol

Calcium handling

High-fat diet

Insulin resistance

LDL receptors

Área de concentração: Fisiologia

Titulação: Doutor em Biologia Funcional e Molecular

Banca examinadora:

Antonio Carlos Boschiero [Orientador]

Angelo Rafael Carpinelli

Marcio Alberto Torsoni

Maria Lucia Bonfleur

Silvana Auxiliadora Bordin da Silva

Data da defesa: 19-03-2012

Programa de Pós Graduação: Biologia Funcional e Molecular

Campinas, 19 de março de 2012

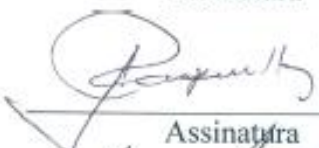
BANCA EXAMINADORA

Profa. Dra. Antonio Carlos Boschiero (Orientador)



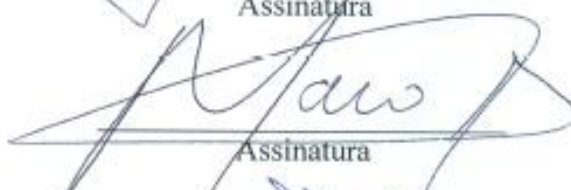
Assinatura

Prof. Dr. Ângelo Rafael Carpinelli



Assinatura

Profa. Dra. Marcio Alberto Torsoni



Assinatura

Profa. Dra. Maria Lucia Bonfleur



Assinatura

Profa. Dra. Silvana Auxiliadora Bordin da Silva



Assinatura

Profa. Dra. Ana Paula Couto Davel

Assinatura

Prof. Dr. Claudio Cesar Zoppi

Assinatura

Profa. Dra. Fernanda Ortis

Assinatura

Dedico este trabalho

*À minha mãe e meu pai pelo imenso amor
e apoio em todos os momentos de minha vida;*

A meu irmão e aos meus sobrinhos.

AGRADECIMENTOS

A Deus por indicar o caminho e dar-me forças para segui-lo;

Ao professor Antonio Carlos Boschiero pela oportunidade oferecida, pelos ensinamentos, por estar sempre presente e pelo exemplo de humildade, respeito e profissionalismo;

À professora Helena Coutinho Franco de Oliveira pela confiança, ensinamentos e pelo constante auxílio no desenvolvimento do trabalho;

Ao professor Everardo Magalhães Carneiro pelo apoio e sugestões valiosas para o desenvolvimento do trabalho;

Aos membros da banca examinadora pelas sugestões e correções no texto final;

Ao Instituto de Biologia da Universidade Estadual de Campinas pela oportunidade profissional;

À Secretaria de pós-graduação em Biologia Funcional e Molecular, em especial à secretária Andrea Ap. V. dos Santos;

Aos funcionários do Departamento de Fisiologia: Alexandra, Lescio Domingos, Marise Mello Carnelossi e Priscila pela atenção e auxílio dispensados sempre que necessário;

À Rosane Aparecida Ribeiro pelos ensinamentos assim que ingressei no doutorado e à Emerielle Cristine Vanzela pelo apoio e dedicação no desenvolvimento de todo trabalho e pela amizade.

Aos colegas do Laboratório de Pâncreas Endócrino e Metabolismo: Ana Paula, André, Adriene, Cláudio, Daniela, Fernanda, Flávia, Gabriel, Gustavo, Helena, Jean, José Maria, Juliana, Junia, Kelly, Luciana, Luiz, Nicoli, Priscila, Rafael, Renato, Sandra, Tarlliza, Thaís, Thiago pela convivência e ajuda sempre que necessário;

À Andressa Coope, Camila Mathias, Camila Oliveira, Lígia Évora, Natália Lysei, Vanessa Araújo pela amizade e companheirismo;

As moradoras do apartamento 53 pela convivência;

À Capes e à FAPESP pelo apoio financeiro;

E a todos que de alguma forma contribuíram para a realização deste trabalho: muito obrigada!

SUMÁRIO

RESUMO.....	ix
ABSTRACT.....	xi
LISTA DE ABREVIATURAS.....	xiii
LISTA DE FIGURAS.....	xvi
LISTA DE TABELAS.....	xix
INTRODUÇÃO.....	20
1. Secreção e ação da insulina.....	20
2. Diabetes Mellitus.....	22
3. A dislipidemia diabética.....	23
4. O modelo animal <i>knockout</i> para o receptor de LDL.....	24
5. Concentrações celulares de colesterol e secreção de insulina.....	25
JUSTIFICATIVA.....	28
OBJETIVOS.....	29
RESULTADOS.....	30
Artigo 1 (Manuscrito submetido): “Cholesterol reduction ameliorates glucose-induced ca ²⁺ handling and insulin secretion in islets from low-density lipoprotein receptor knockout mice”.....	31
Abstract.....	32
Introduction.....	33
Material and methods.....	34
Results.....	37
Discussion.....	39
References.....	42
Figures.....	45
Artigo 2: “Insulin action in LDL receptor knockout mice (LDLR ^{-/-}) fed chow or high-fat diet”.....	54
Abstract.....	55
Introduction.....	56
Material and methods.....	57
Results.....	59

Discussion.....	61
References.....	63
Tables.....	66
Figures.....	68
CONCLUSÃO GERAL.....	74
REFERÊNCIAS.....	75
ANEXOS.....	83
I. Comitê de ética experimental.....	83
II. Comitê de Biossegurança.....	84

RESUMO

Alterações no conteúdo de colesterol celular podem contribuir para o mau funcionamento das células-beta pancreáticas. Camundongos *knockout* para o receptor de LDL ($\text{LDLR}^{-/-}$) possuem maior teor de colesterol nas ilhotas pancreáticas e secretam menos insulina em comparação a camundongos selvagens (WT). Neste estudo, investigamos a associação entre o conteúdo de colesterol, a secreção de insulina e a movimentação de cálcio citoplasmático nessas ilhotas. Além disso, analisamos o efeito da dieta rica em gordura (HFD) sobre a homeostasia glicêmica, secreção e ação da insulina nesses camundongos. Os resultados mostraram que a primeira e segunda fase de secreção de insulina assim como a movimentação de Ca^{2+} , estimuladas por glicose, foram reduzidas nos $\text{LDLR}^{-/-}$. Camundongos $\text{LDLR}^{-/-}$ também apresentaram menor conteúdo de proteínas envolvidas com a extrusão dos grânulos de insulina tais como: VAMP-2 e SNAP-25 ($p<0,05$). A remoção do excesso de colesterol pelo uso da metil-beta-ciclodextrina ($\text{M}\beta\text{CD}$) normalizou a secreção de insulina, estimulada por glicose (GSIS) ou tolbutamida, assim como a movimentação de cálcio estimulada por glicose. A remoção do colesterol das ilhotas WT com 0.1 e 1 mmol/L de $\text{M}\beta\text{CD}$ reduziu a secreção bem como a movimentação de cálcio. No entanto, ilhotas incubadas com 10 mmol/L de $\text{M}\beta\text{CD}$ apresentaram aumento significativo na secreção de insulina, apesar da redução na movimentação de cálcio. A dieta hiperlipídica (H) promoveu maior ganho de peso e acúmulo de gordura visceral nos camundongos $\text{LDLR}^{-/-}\text{H}$ em relação aos WTH. A dieta aumentou a glicemia tanto no jejum quanto alimentado, porém não houve alterações nas concentrações plasmáticas de insulina nos camundongos $\text{LDLR}^{-/-}\text{H}$. Já nos camundongos WTH, a dieta causou aumento nas glicemias de jejum e alimentado bem como na insulinemia. A área sob a curva glicêmica durante o oGTT foi 30% maior nos camundongos $\text{LDLR}^{-/-}\text{H}$. A GSIS não foi significativamente alterada pela dieta hiperlipídica em ambos os grupos. Camundongos $\text{LDLR}^{-/-}$ em dieta padrão apresentaram maior fosforilação do receptor de insulina ($\text{IR}\beta$) e da AKT em fígado e músculo. O conteúdo da enzima que degrada a insulina (IDE) se mostrou reduzido nos $\text{LDLR}^{-/-}$. A dieta hiperlipídica reduziu a sinalização da insulina em fígado, músculo e tecido adiposo dos camundongos $\text{LDLR}^{-/-}\text{H}$. Nos camundongos WTH essa dieta promoveu apenas uma redução na fosforilação do $\text{IR}\beta$ no músculo. A análise conjunta dos resultados nos permitiu concluir que, tanto o aumento de colesterol verificado em ilhotas $\text{LDLR}^{-/-}$ quanto a diminuição excessiva do conteúdo de colesterol em ilhotas WT (tratadas

com M β CD) alteram a movimentação de cálcio e consequentemente a secreção de insulina. A redução do colesterol nas ilhotas dos camundongos LDLR^{-/-} corrigiu a redução da secreção de insulina, apesar das concentrações reduzidas de VAMP-2 e SNAP-25. Camundongos LDLR^{-/-}, alimentados com dieta padrão, são mais sensíveis à insulina, provavelmente como um mecanismo adaptativo a menor secreção de insulina. No entanto, estas adaptações não são suficientes para manter a homeostase glicêmica visto que estes animais são intolerantes à glicose. Quando alimentados com dieta hiperlipídica, os LDLR^{-/-}H se tornam resistentes à insulina provavelmente devido ao aumento do tecido adiposo visceral.

ABSTRACT

Changes in cellular cholesterol levels may contribute to beta cell dysfunction. Islets from LDL receptor knockout ($\text{LDLR}^{-/-}$) possess higher cholesterol content and secrete less insulin than wild type (WT) mice. Here, we investigated the association between cholesterol content, insulin secretion and Ca^{2+} handling in these islets. In addition, we analyzed the effects of high-fat-diet (HFD) on glucose homeostasis, insulin secretion and action in these mice. Both first and second phase of glucose-stimulated insulin secretion (GSIS) were lower in $\text{LDLR}^{-/-}$ compared with WT islets. This lower secretion was paralleled by impairment in Ca^{2+} handling in these islets. The contents of SNAP-25 and VAMP-2 proteins, which participate in the extrusion of the insulin containing granules, were reduced in $\text{LDLR}^{-/-}$ compared with WT islets. Removal of the excess of cholesterol from $\text{LDLR}^{-/-}$ islets (Methyl- β -cyclodextrine, M β CD) normalized glucose- and tolbutamide-induced insulin release. Glucose-stimulated Ca^{2+} handling was also normalized in cholesterol-depleted $\text{LDLR}^{-/-}$ islets. Cholesterol removal from WT islets by 0.1 and 1.0 mmol/L M β CD impaired both GSIS and Ca^{2+} handling. However, 10 mmol/L M β CD markedly increased insulin secretion induced by glucose or tolbutamide in WT islets, despite a significant reduction in Ca^{2+} handling. The HFD promoted higher body weight gain and visceral fat pad depot in $\text{LDLR}^{-/-}\text{H}$ than in WTH. $\text{LDLR}^{-/-}\text{H}$ mice showed fasted and fed glucose levels significantly higher whereas no changes in fasted plasma insulin levels were observed. WTH mice also showed an increase in fasted and fed glucose levels, but a higher fasted plasma insulin level ($p < 0.05$) was noticed. The area under the curve of the oGTT in $\text{LDLR}^{-/-}\text{H}$, but not in WTH, was increased (30%) by HFD. GSIS was not significantly altered by HFD in both groups. $\text{LDLR}^{-/-}$ mice showed higher IR β and AKT phosphorylation in liver and skeletal muscle. Insulin degrading enzyme (IDE) protein content was lower in liver of $\text{LDLR}^{-/-}$. The HFD reduced insulin signaling in liver, skeletal muscle and adipose tissue in $\text{LDLR}^{-/-}\text{H}$. In WTH the HFD reduced only the IR β phosphorylation in muscle. In conclusion, our results indicate that abnormal high ($\text{LDLR}^{-/-}$ islets) or low (WT islets treated with M β CD) cholesterol contents alter both GSIS and Ca^{2+} handling. Normalization of islet cholesterol content improved Ca^{2+} handling and insulin secretion in $\text{LDLR}^{-/-}$ islets, despite the lower expression of SNAP-25 and VAMP-2. $\text{LDLR}^{-/-}$ mice, fed a chow diet, are more sensitive to insulin probably due adaptive mechanisms that compensate the low insulin secretion. However, these changes are not sufficient to promote glucose

homeostasis since these mice were glucose intolerants. When fed a high-fat diet, they became also insulin resistant probably due to an increase in the mass of the visceral adipose tissue.

LISTA DE ABREVIATURAS

- ABCA-1** - *ATP-binding cassette, sub-family A member 1*
- ABCG-1** - *ATP-binding cassette, sub-family G member 1*
- AGL** - Ácidos graxos livres
- ADP** - Adenosina difosfato
- AKT** – cinase serina/treonina dependente de fosfatidilinositol-3-cinase
- AMPc** - Adenosina monofosfato cíclico
- Apo-E** - Apoliproteína E
- ATP** - Adenosina trifosfato
- Apo** - Apoliproteínas
- bHLH** - *basic helix-loop-helix*
- Ca²⁺** - Cálcio
- [Ca²⁺]** - Concentração intracelular de cálcio
- CE** - Ésteres de colesterol
- CHOL** - Colesterol
- CL** - Colesterol livre
- COA** - Coenzima-A
- COL** - Colesterol
- COPII** - *Coat Protein II*
- CO₂** - Dióxido de carbono
- DM** - Diabetes mellitus
- DM1** - Diabetes mellitus tipo I
- DM2** - Diabetes mellitus tipo II
- EDTA** - Ácido etilenodiamino tetra-acético
- GSIS** - Secreção de insulina estimulada pela glicose
- HFD** – High-fat diet (dieta hiperlipídica)
- HDL** - Lipoproteína de alta densidade
- HMG-CoA** - 3-hidroxi-3-metil-glutaril coenzima A
- IDE** - *Insulin degrading enzyme*
- IKKβ** - *Inhibitor of nuclear factor kappa-B kinase*

iNOS - Enzima Óxido Nítrico Sintase Induzível

INSIG – *Gene induzido pela insulina*

IP3 - Inositol 1,4,5-trifosfato

IR - Receptor de insulina

IR β - Subunidade beta do receptor de insulina

JNK - *Junc kinase*

KRBB – Tampão Krebs- Ringer-bicarbonato

LCAT - Lecitina colesterol acil transferase

LDL- Lipoproteína de baixa densidade

LDLR - Receptor de LDL

LDLR^{-/-} - Camundongos *knockout* para o LDLR

LDLR^{-/-}H - Camundongos LDLR^{-/-} alimentados com dieta hiperlipídica

LP - Lipoproteína

LPL - Lipoproteína lipase

LRP - *LDL receptor related protein*

M β CD - Metil-beta-ciclodextrina

NB598 – Bloqueador farmacológico da enzima esqualeno epoxidase

NEFA- *Non-esterified fatty acids*

oGTT -Teste de tolerância oral a glicose

PKA - Proteína cinase A

PKC - Proteína cinase C

PMSF - *Phenylmethylsulfonylfluoride*

PTP1B - Proteína tirosina fosfatase 1B

QM - Quilomícrons

RIA - Radioimunoensaio

RXR - *Retinoid X receptor*

S1P - *Membrane-bound transcription factor peptidase site1*

S2P - *Membrane-bound transcription factor peptidase site2*

SCAP - *SREBP cleavage-activating protein*

SR-B1 – *Scavenger receptor class B type1*

SREBP - *Sterol regulatory element binding protein*

SNAP-25 – Proteína associada à sinaptossomal 25

SNARE – *soluble N-ethylmaleimide-sensitive factor attachment protein receptors*

TG – Triglicérides

t-SNARE – Target SNARE

Tyr - Tirosina

VAMP2 – Proteína associada à membrana de vesícula 2

VGCC - Canal de cálcio voltagem-dependente

VLDL - Lipoproteína de densidade muito baixa

v-SNARE – Vesicle-SNARE

WT - Camundongos wild-type (C57Bl6)

WTH - Camundongos wild-type alimentados com dieta hiperlipídica

LISTA DE FIGURAS

Figura 1. Síntese de colesterol. Resumo das etapas principais da síntese de colesterol a partir da acetil-coenzima-A. Adaptado de Lehninger, Nelson e Cox, 2006.....26

ARTIGO I

Figure 1. Effects of 11.1 mmol/l glucose on the dynamics of insulin release from WT (open squares and open bars) and LDLR^{-/-} (solid circles and dark bars) mice islets. Groups of 50 freshly isolated islets were perfused for 80 min (A). Glucose at 2.8 mmol/l was present from the onset of the experiment and was increased to 11.1 mmol/l from min 16 until the end of the perfusion period. Cumulative insulin release during the first phase (B), measured as AUC1 between time points t=16 and 22 min, and summed insulin release during the second phase (AUC2), measured between time points t= 23 and 80min (C). Values are means±SEM of four distinct experiments. *p<0.05 vs. WT.....45

Figure 2. Representative curves of changes in intracellular Ca²⁺ concentrations in response to 11.1 mmol/l glucose in WT (solid line and open bars) and LDLR^{-/-} (dotted lines and dark bars) mice islets (A). The Area Under the Curves (AUC) was calculated for 3 different periods at 11.1 mmol/l glucose: B (1-15 min), C (1-6 min), and D 6-15 min of perfusion. Values are the ratios of F340/F380 registered for each group. Data are means ± SEM of 4 independent experiments. *p<0.05 indicates significant difference vs WT.....46

Figure 3. Tolbutamide (100 µmol/l) induced Ca²⁺ rise in WT (solid line and open bar) and LDLR^{-/-} (dotted line and dark bar) mice islets (A). The Area Under the Curves (AUC) was calculated when tolbutamide was present in the perfusion period (B). Values are the ratios of F340/F380 registered for each group. Data are means ± SEM from 7 independent experiments. *p<0.05 indicates significant difference vs WT.....47

Figure 4. SNAP-25 (A), VAMP-2 (B) and Syntaxin-1A (C), protein expression in isolated islets from WT (open bars) and LDLR^{-/-} (dark bars) mice. Protein extracts were processed for

Western blotting. The bars represent the means \pm SEM of the values, determined by optical densitometry. n = (3-5). *p<0.05 vs WT.....48

Figure 5. Cholesterol levels from WT (open bars) and LDLR^{-/-} (dark bars) mice islets. Cholesterol depletion was done by incubating the islets in the presence of increasing concentrations of M β CD for 1 h at 37°C. Values represent means \pm SEM *p<0.05 compared WT (without M β CD); $^{\#}$ p<0.05 compared LDLR^{-/-} (without M β CD).....49

Figure 6. Effects of M β CD treatment on glucose induced [Ca $^{2+}$]i rise in WT and LDLR^{-/-} mice islets. (A) Representative curves of changes in intracellular Ca $^{2+}$ concentrations in response to 11.1 mmol/l glucose in WT islets; WT (line with solid squares), WT+0.1mmol/l M β CD (line with open circles), WT+1mmol/l M β CD (dotted line), and WT+10mmol/l M β CD (solid line). (B) Representative curves of changes in intracellular Ca $^{2+}$ concentrations in response to 11.1 mmol/l glucose in LDLR^{-/-} islets; LDLR^{-/-} (line with solid squares), LDLR^{-/-}+0.1mmol/l M β CD (line with open circles), LDLR^{-/-}+1mmol/l M β CD (dotted line), and LDLR^{-/-}+10mmol/l M β CD (solid line). (C) AUC from glucose induced calcium rise. Values are the ratios of F340/F380 registered for each group. Data are means \pm SEM for 4-9 independent experiments. * P < 0.05 compared WT (without M β CD); $^{\#}$ P < 0.05 compared LDLR^{-/-} (without M β CD); $^{\$}$ P < 0.05 compared WT (without M β CD) by one-way ANOVA; & < 0.05 compared LDLR^{-/-} (without M β CD) by one-way ANOVA.....50

Figure 7. Effects of cholesterol depletion on the glucose-induced insulin secretion by WT (open bars) and LDLR^{-/-} (dark bars) mice islets. Cholesterol depletion was done by incubating the islets in the presence of increasing concentrations of M β CD for 1 h at 37°C. Each bar represents mean \pm SEM of 12-20 groups of islets from 6 different mice. *p<0.05 vs. WT; **p<0.01 vs WT; $^{\#}$ p<0.05, vs LDLR^{-/-}.....51

Figure 8. Effects of M β CD treatment on tolbutamide-induced [Ca $^{2+}$]i rise in WT and LDLR^{-/-} mice islets. (A) Representative curves of changes in intracellular Ca $^{2+}$ concentrations in response to tolbutamide in WT islets; WT (solid line), WT+1mmol/l M β CD (dotted line), and WT+10mmol/l M β CD (line with open circles), and LDLR^{-/-} islets (B): LDLR^{-/-} (solid line),

LDLR^{-/-} +1mmol/l MβCD (dotted line), and LDLR^{-/-} +10mmol/l MβCD (line with open circles). (C) Area under de curve (AUC) from tolbutamide induced calcium rise. Values are the ratios of F340/F380 registered for each group. Data are means±SEM from 5-7 independent experiments. *p<0.05 vs WT (without MβCD); **p<0.01 vs WT (without MβCD); # p<0.05 compared LDLR^{-/-} (without MβCD).....52

Figure 9. Effects of cholesterol depletion on the tolbutamide-induced insulin secretion in WT (open bars) and LDLR^{-/-} (dark bars) mice islets. Cholesterol depletion was done by incubating the islets in the presence of increasing concentrations of MβCD for 1 h at 37°C. Each bar represents mean ± SEM of 10-16 groups of islets from 6 different mice. *p<0.05 vs. WT (without MβCD); **p<0.01 vs WT (without MβCD); #p<0.05, vs LDLR^{-/-} (without MβCD).53

ARTIGO 2

Figure 1. (A) – Blood glucose during a glucose tolerance test (oGTT) in WT (solid squares), WTH (open squares), LDLR^{-/-} (solid circles) e LDLR^{-/-H} (open circles). (B) - Area under the curve (AUC) during the oGTT test. The bars represent means ± SEM of the AUC of each mice, n=8-10. *p<0.05 compared WT; # p<0.05 compared LDLR^{-/-}68

Figure 2. Insulin secretion stimulated by 2.8mmol/L and 11.1 mmol/L of glucose. Bars represent means ± SEM of the 12-20 groups of islets of 6 different mice. * vs WT p < 0,05..69

Figure 3. Insulin signaling in liver of mice fed chow diet (WT e LDLR^{-/-}) and high-fat-diet (WTH e LDLR^{-/-H}). A. Imunoprecipitation (IP) with α-IRβ (IRβ) and imunoblotting (IB) with α-phosphorylated-tyrosine (pTyr) or α-IRβ antibodies. B. Imunoblotting with α-phosphorylated-AKT (pAKT). C. Imunoblotting with α-AKT1/2/3 (AKT). The bars represent means ± SEM of the values determined by optical densitometry. n = (4-5). * p<0.05 compared WT stimulated with exogenous insulin; # p<0.05 compared LDLR^{-/-} stimulated with exogenous insulin.....70

Figure 4. Insulin signaling in gastrocnemius muscle of mice fed chow diet (WT e LDLR^{-/-}) and high-fat diet (WTH e LDLR^{-/-H}). A. Imunoprecipitation (IP) with α-IRβ (IRβ) and

imunoblotting (IB) with α -phosphorylated-tyrosine (pTyr) or α -IR β antibodies. B. Imunoblotting with α -phosphorylated-AKT (pAKT). C. Imunoblotting with α -AKT1/2/3 (AKT). The bars represent means \pm SEM of the values determined by optical densitometry. n = (3-5). * p<0.05 compared WT stimulated with exogenous insulin; # p<0.05 compared LDLR $^{-/-}$ stimulated with exogenous insulin.....71

Figure 5. Insulin signaling in adipose tissue of mice fed chow diet (WT e LDLR $^{-/-}$) and high-fat-diet (WTH e LDLR $^{-/-}H$). A. Imunoprecipitation (IP) with α -IR β (IR β) and imunoblotting (IB) with α -phosphorylated-tyrosine (pTyr) or α -IR β antibodies. B. Imunoblotting with α -phosphorylated-AKT (pAKT). C. Imunoblotting with α -AKT1/2/3 (AKT). The bars represent means \pm SEM of the values determined by optical densitometry. n = (4-5). & p<0.05 compared WT without exogenous insulin stimulus; # p<0.05 compared LDLR $^{-/-}$ stimulated with exogenous insulin.....72

Figure 6. Insulin-degrading-enzyme (IDE) protein expression in liver from WT (open bars) and LDLR $^{-/-}$ (dark bars), WTH (bars with horizontal lines) and LDLR $^{-/-}H$ (bars with vertical lines) mice. Protein extracts were processed for Western blotting. The bars represent means \pm SEM of the values determined by optical densitometry. n = (5). * p<0.05 compared WT; # p<0.05 compared LDLR $^{-/-}$73

LISTA DE TABELAS

ARTIGO 2

Table 1 – Composition of high-fat diet.....66

Table 2. Body weight, epididymal and retroperitoneal fat depot in mice fed with chow diet (WT e LDLR $^{-/-}$) and high-fat diet (WTH e LDLR $^{-/-}H$).....66

Table 3. Glucose, insulin and plasma lipids in mice fed with chow diet (WT e LDLR $^{-/-}$) and high-fat diet (WTH e LDLR $^{-/-}H$).....67

INTRODUÇÃO

1. Secreção e ação da insulina

A secreção de insulina pelas células β pancreáticas é regulada por fatores metabólicos, neurais e endócrinos. Os dois últimos participam da potencialização ou da inibição da liberação de insulina atuando apenas quando a secreção já foi iniciada. Os fatores metabólicos são os responsáveis por estimular a secreção da insulina. Dentre estes fatores a glicose é o mais importante agente estimulador [1]. A glicose penetra nas células β pancreáticas através do transportador GLUT-2, localizado na membrana destas células. Após ser internalizada a glicose é fosforilada pela glicoquinase e metabolizada na via glicolítica e no ciclo de Krebs o que gera um aumento na concentração de ATP que altera a razão ATP/ADP no interior da célula [1, 2]. Este aumento na razão ATP/ADP induz o fechamento de canais de K^+ sensíveis ao ATP, diminuindo o efluxo deste íon, e promovendo, consequentemente, despolarização da membrana, abertura de canais de Ca^{2+} voltagem dependentes (VDGC) e o influxo dos íons Ca^{2+} [3].

A metabolização da glicose nas células β e o consequente aumento na concentração de cálcio intracelular leva a ativação de enzimas que produzem mensageiros intracelulares que contribuem para a amplificação do sinal iniciado pela glicose [4]. Uma destas enzimas é a adenilato ciclase, que ao clivar o ATP, produz adenosina monofosfato cíclico (AMPc) que, por sua vez, estimula a proteína quinase A (PKA) [5, 6]. Além disso, a metabolização da glicose também estimula a hidrólise de fosfoinosítideos através da ativação da fosfolipase C (PLC) resultando na formação do inositol-1,4,5-trifosfato (IP3) e diacilglicerol (DAG). O IP3 se difunde pelo citoplasma e induz a liberação de Ca^{2+} de estoques intracelulares aumentando sua concentração citoplasmática, enquanto o DAG estimula a proteína quinase C (PKC) [4]. Todos estes eventos induzidos pela metabolização da glicose (aumento citoplasmático de Ca^{2+} e ativação da PKA, PLC e PKC) culminam com a exocitose dos grânulos secretórios contendo insulina [7, 8].

Além da glicose, nutrientes como ácidos graxos e aminoácidos podem influenciar a secreção de insulina [7, 9]. Com relação aos aminoácidos, sabe-se que os aminoácidos essenciais em condições que mimetizam as fisiológicas, aumentam a resposta secretória da célula β [10] e em concentrações suprafisiológicas aminoácidos individuais exercem diversas ações sobre o processo de síntese e secreção de insulina [9]. Já os ácidos graxos livres podem

estimular ou inibir a secreção de insulina dependendo principalmente de concentração e tempo de exposição das células beta a estes nutrientes.

Hormônios intestinais como GLP-1 (glucagon like peptide 1) e o peptídeo gástrico insulinotrópico (GIP), liberados no período pós-alimentar potencializam a secreção de insulina. Outros hormônios, produzidos pelas ilhotas pancreáticas como o glucagon e a somatostatina exercem efeitos parácrinos sobre a secreção de insulina [11]. Finalmente, o sistema nervoso autonômico possui um papel importante na modulação da secreção de insulina. O sistema nervoso parassimpático, através de receptores muscarínicos, potencializa a secreção da insulina, enquanto o sistema nervoso simpático, agindo por meio de receptores adrenérgicos, inibe a secreção de insulina [12, 13].

De modo geral, a insulina liberada estimula processos anabólicos de armazenamento de reservas energéticas, isto é, promove a síntese de glicogênio, lipídios e proteínas, agindo principalmente nos músculos, no tecido adiposo e no fígado. No fígado, a insulina estimula a síntese de glicogênio, através da ativação de enzimas principalmente a glicogênio sintetase, e diminui a produção de glicose por inibir a gliconeogênese e a glicogenólise. A insulina também aumenta a captação de glicose, principalmente no músculo esquelético e no tecido adiposo, bem como promove síntese e inibe a degradação de proteínas. No tecido adiposo a insulina também é responsável estimular a lipogênese e inibir a lipólise [14, 15].

As ações da insulina nos tecidos alvo ocorrem por meio de sua ligação com a subunidade α do receptor de insulina (IR), que apresenta atividade tirosina cinase intrínseca. O resultado da interação entre o hormônio e o IR é uma mudança conformacional do mesmo, que estimula a autofosforilação de vários resíduos tirosina nas subunidades β do IR e a fosforilação em tirosina dos substratos do IR (IRS), os quais ancoram proteínas que possuem um sítio específico para o acoplamento com outros sinalizadores intracelulares que apresentam o domínio SH2 (assim denominados devido à homologia com o produto do oncogene *src*). A ligação dos domínios SH2 da fosfatidilinositol-3-cinase aos resíduos fosfotirosinas do IRS-1 ativa esta enzima, que produz fosfolipídeos de fosfatidilinositol (PI), dentre eles o PI(3,4,5)-trifosfato, que ativa a proteína cinase dependente de PI, e subsequentemente a Akt. Esta serina/treonina cinase fosforila várias proteínas, dentre as quais, proteínas relacionadas à translocação de GLUT4 para a membrana plasmática. Além disso, a AKT também fosforila e inibe a enzima GSK3 (cinase da glicogênio-sintase-3) o que resulta no aumento na síntese de

glicogênio. Em relação ao metabolismo lipídico, a AKT estimula a transcrição de enzimas relacionadas com a lipogênese e, em contrapartida, inibe a lipólise por ativar fosfodiesterases, inibindo a lipase hormônio sensível [16-19].

A perda da eficiência da insulina em promover seus efeitos fisiológicos é denominada resistência periférica a ação da insulina [20]. Várias alterações moleculares e funcionais estão relacionadas ao desenvolvimento da resistência a insulina, como por exemplos: diminuição na concentração do IR e seus substratos (IRS), diminuição na atividade cinase dos receptores, aumento nas fosfatases que desfosforilam o IR e demais proteínas da via de sinalização. Tanto fatores genéticos quanto ambientais contribuem para o aparecimento do quadro de resistência a insulina [20, 21]. Clínica e experimentalmente é observada uma forte correlação entre obesidade, distúrbios no metabolismo lipídico, resistência a insulina e desenvolvimento do diabetes mellitus do tipo II. [22-24].

2. O diabetes mellitus

As células β pancreáticas secretam insulina em resposta ao aumento da concentração de glicose sanguínea. Em circunstâncias normais, a glicose liberada na corrente sanguínea é rapidamente captada pelos tecidos através da ação da insulina [25]. O Diabetes Mellitus (DM) é uma doença metabólica caracterizada por defeitos na secreção e/ou ação da insulina, com consequente aumento da glicemia [26].

O DM é considerado um grave problema de Saúde Pública que, segundo estimativas da Organização Mundial de Saúde, atingirá mais de 300 milhões de pessoas ao redor do mundo até 2030 [27]. O DM se divide em dois tipos principais: o Tipo I e o Tipo II. O DM tipo 1 (DM1), corresponde a 5% a 10% dos casos, resulta da destruição das células beta pancreáticas com consequente deficiência de insulina. Na maioria dos casos, a destruição destas células é mediada por auto-imunidade, porém existem casos em que não há evidências de processo auto-imune, sendo, portanto, referida como forma idiopática do DM1 [26, 28]. O DM tipo 2 (DM2), forma mais comum da doença (90% a 95% dos casos), é uma patologia complexa determinada pela interação de fatores genéticos e ambientais, caracterizada por defeitos na ação e na secreção da insulina [26, 28, 29]. Além das alterações glicêmicas,

pacientes DM2 apresentam, com freqüência, modificações no perfil lipídico, quadro clinicamente denominado como dislipidemia diabética [30].

3. A dislipidemia diabética

A dislipidemia diabética caracteriza-se por aumento na concentração plasmática de triglicerídeos (TG) [31], diminuição das lipoproteínas de alta densidade (HDL) e aumento e modificações químicas nas lipoproteínas de baixa densidade (LDL) [32-34]. Durante muitos anos a dislipidemia diabética foi considerada apenas como uma consequência da resistência à ação da insulina, no entanto, estudos epidemiológicos vêm demonstrando que alterações nos lipídeos plasmáticos precedem as manifestações clínicas do DM2 [35, 36]. Deste modo, a dislipidemia passou a ser considerada também como uma causa da patogênese do DM2. Estudos mais recentes em diferentes modelos experimentais, células beta pancreáticas isoladas de camundongos e ilhotas humanas indicam uma função importante das lipoproteínas na patogênese da resistência a insulina assim como na sobrevivência e função secretora das células beta [37-39].

Ilhotas isoladas e incubadas com LDL apresentam uma redução na secreção de insulina estimulada por glicose sem alteração do conteúdo de RNAm e de insulina [39]. No entanto, a exposição prolongada de células beta à LDL oxidadas diminui a transcrição da preproinsulina, por ativação da C-Junc-N-terminal kinase (JNK). A ativação da JNK pelas LDL oxidadas também induzem apoptose em células beta. Ambos os efeitos podem ser revertidos pela adição das HDL [40]. Além disso, a adição de HDL em culturas de células beta diminui a apoptose induzida por privação de nutrientes, altas concentração de glicose e citocinas pró-inflamatórias [38, 39, 41]. Estes efeitos estão relacionados à diminuição da clivagem da caspase-3 e à *dowregulation* do receptor de TNF e da enzima Óxido nítrico sintase induzível (iNOS) [38]. Além disso, as HDL aumentam a proliferação das células beta por ativar a AKT [14]. Estes resultados sugerem que tanto aumento das LDL oxidadas quanto diminuição nas concentrações de HDL, observados em pacientes com DM2, podem contribuir para piora no funcionamento das células beta.

4. O modelo animal *knockout* para o receptor de LDL

Os modelos animais geneticamente modificados para superexpressar ou não expressar (*knockout*) genes específicos envolvidos no transporte intravascular de lipídeos tem sido muito úteis para as investigações das repercussões metabólicas e patológicas das dislipidemias genéticas [42, 43]. Animais *knockout* para o LDLR [44] apresentam o fenótipo de hipercolesterolemia familiar, uma doença genética com alta frequência na forma heterozigótica (1:500) na população ocidental, caracterizada por altos níveis de LDL-colesterol [45].

Camundongos que não expressam receptor de LDL alimentados com dieta pobre em gordura apresentam concentração de colesterol plasmático 2 a 4 vezes maior quando comparados aos camundongos selvagens. Quando submetidos à dieta rica em gordura, estes camundongos desenvolvem aterosclerose e xantomatoze severas [46, 47], hipertrigliceridemia [48] obesidade e hiperglicemias [49].

Foi demonstrado que mitocôndrias dos camundongos $\text{LDLR}^{-/-}$ produzem maior quantidade de espécies reativas de oxigênio (EROS) e desenvolvem mais transição de permeabilidade de membrana, um processo que desencadeia morte celular, seja por necrose ou por apoptose [50]. Este aumento na produção de EROS não foi relacionado a alterações de conteúdo de colesterol na membrana, fluidez da membrana ou atividade da superóxido dismutase mitocondrial, mas sim a um menor conteúdo de NADPH, que corresponde à principal fonte de equivalentes redutores para o sistema enzimático antioxidante mitocondrial. Foi proposto que a maior lipogênese e esteroidogênese verificadas nestes animais (para compensar a menor captação de LDL) seriam responsáveis pela menor disponibilidade de NADPH, levando à condição de estresse oxidativo nas células destes animais [51].

Em relação ao metabolismo glicêmico, nosso grupo demonstrou que na ausência de dieta rica em gordura, os camundongos $\text{LDLR}^{-/-}$ apresentaram redução na tolerância à glicose associada à redução na secreção de insulina em resposta à concentração pós-prandial de glicose [52]. As ilhotas destes camundongos também apresentam maior conteúdo de colesterol [52] e produção reduzida de CO_2 derivado da glicose, possivelmente devido ao aumento da demanda do substrato para sustentar à esteroidogênese [51].

5. Concentrações celulares de colesterol e secreção de insulina

As concentrações celulares de colesterol são controladas por um balanço entre a síntese intracelular e captação de colesterol do plasma, de um lado, versus o efluxo de colesterol dos tecidos, de outro. O colesterol é fornecido para as células através de duas rotas: uma via de biossíntese “de novo” colesterol a partir de acetil-coenzima A (CoA) e, outra via extracelular, mediada pela endocitose de lipoproteínas (LDL) via LDLR [53].

Todas as células nucleadas são capazes de sintetizar colesterol a partir da acetil-coenzima A, através de um processo multi-enzimático que ocorre no retículo endoplasmático, o qual tem como passo limitante a conversão da HMG-CoA em mevalonato pela ação da enzima HMG-CoA redutase (figura 1). Todas as células de mamíferos também são capazes de captar colesterol exógeno através da internalização das LDL via LDLR [54]. Por outro lado, o efluxo do colesterol dos tecidos, chamado transporte reverso de colesterol, é mediado pelos receptores ABCA-1 e ABCG-1, localizadas nas membranas celulares. Os receptores ABC interagem com as Apolipoproteínas A-1 das HDLs transferindo o colesterol celular para esta lipoproteína. As HDLs, por sua vez, transportam o colesterol novamente para o fígado onde este é captado pelos receptores SR-B1 [55].

Os processos de síntese, captação e processamento do colesterol são regulados por dois sistemas de receptores nucleares: os *Sterol Regulatory Element Binding Protein* (SRBPs) e os *Liver-X-receptors* (LXR). A família dos fatores de transcrição SREBPs regulam a expressão de genes relacionados ao metabolismo lipídico, e o SREBP-2 é o principal regulador dos genes relacionados a metabolismo de colesterol, como HMG-CoA redutase e LDLR. Quando as concentrações intracelulares de colesterol estão altas uma proteína de membrana do retículo endoplasmático, denominada SREBP, encontra-se inativa e ligada à outra proteína chamada SCAP (*SREBP cleavage-activating protein*) que atua como um sensor da quantidade de colesterol nas membranas. Quando a concentração de colesterol nas membranas diminui ocorre uma mudança conformacional na proteína SCAP que permite que o complexo SCAP-SREBP se desligue da proteína INSIG (*insulin-induced gene*) e se associe a vesículas contendo COPII, as quais migram para o complexo de Golgi. No complexo de Golgi, a SREBP é clivada seqüencialmente por duas diferentes proteases. A primeira clivagem é catalisada por uma serina-protease (S1P) ligada à membrana que cliva a SREBP no lado luminal. Em seguida, uma metaloprotease, também ligada à membrana (S2P), cliva o primeiro

domínio transmembrana da SREBP próximo a interface com o citoplasma, liberando a porção amino-terminal da SREBP que pertence a família de fatores de transcrição bHLH (*basic helix-loop-helix*). Esse domínio constitui a SREBP ativa que transloca-se para o núcleo e estimula a transcrição dos genes que aumentam a síntese e a captação de colesterol, como do receptor da LDL, da HMG-CoA redutase e outros genes responsivos ao colesterol [57-59].

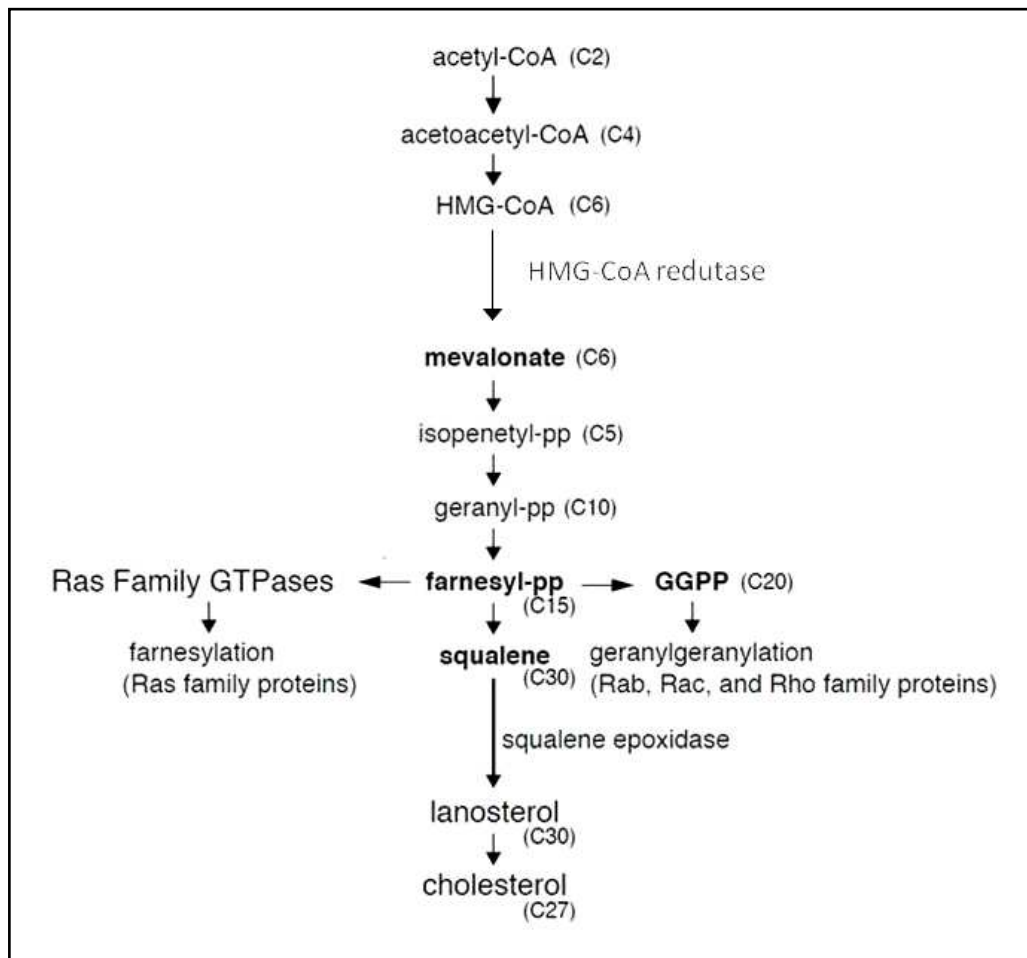


Figura 1. Síntese de colesterol. Resumo das etapas principais da síntese de colesterol a partir da acetil-coenzima-A. (adaptado de Lehninger, Nelson e Cox, 2006) [56].

A expressão dos transportadores ABCA1 e ABCG1 (responsáveis pelo efluxo de colesterol das células), por sua vez, é regulada positivamente por mecanismos transcricionais e pós-transcpcionais. A entrada do colesterol advindo das LDL gera óxidos de colesterol que são ligantes naturais dos LXR. O LXR se acopla ao receptor de ácido retinóico RXR, e o complexo LXR/RXR liga-se diretamente ao ABCA1. Quando o conteúdo celular de esteróides

é baixo, o complexo ABCA1-LXR/RXR permanece ligado à membrana; porém com o acúmulo de colesterol os óxidos de colesterol se ligam ao LXR, com dissociação do ABCA-1, o qual passa a intermediar o efluxo de colesterol para as Apo-1 [60]. O rompimento de qualquer componente destas vias pode levar a drásticas mudanças nas concentrações celulares de colesterol e, consequentemente, nas funções das células.

O colesterol constitui aproximadamente 20% do total dos lipídeos das células beta e é essencial para a manutenção da estrutura e organização da membrana destas células [61, 62]. Devido a sua estrutura química o colesterol se associa aos esfingolipídeos e formam regiões nas membranas conhecidas como balsas lipídicas (*lipid rafts*) [63]. Numerosas proteínas de membrana estão associadas a estes microdomínios como, por exemplo, os canais de cálcio e de potássio [64-66]. Nestes domínios também se associam proteínas que estão envolvidas no processo de exocitose dos grânulos de insulina como, por exemplo, as proteínas membros da superfamília das SNARE (*soluble N-ethylmaleimide-sensitive factor attachment protein receptors*) [67, 68]. O conteúdo de colesterol nestes microdomínios é essencial para manter a associação entre o estímulo secretório, que ocorre com a entrada de cálcio pelos canais de cálcio voltagem dependentes, e as proteínas SNARE que medeiam a exocitose do grânulo e consequentemente secreção de insulina [66-68].

Camundongos transgênicos que superexpressam o SREBP-2 especificamente em células beta desenvolvem diabetes severo com redução da massa e funcionalidade destas células. Comparados aos animais controle (C57Bl6) estes camundongos apresentam um pâncreas de tamanho reduzido e com menor número de ilhotas. Estas mudanças nas características fenotípicas dos animais se devem ao acúmulo de colesterol nas células beta, o qual leva a uma diminuição na expressão de fatores de transcrição como o PDX-1 e BETA-2, ambos importantes para o desenvolvimento e sobrevivência celulares [69].

O acúmulo de colesterol nas células beta pancreáticas interfere diretamente no processo de secreção de insulina, estimulada pela glicose. Camundongos deficientes de apolipoproteína-E (Apo-E) apresentam maior teor de colesterol nas ilhotas e secretam menos insulina tanto em condições basais quanto estimulatórias [70]. Além disso, camundongos knockout-específicos para o receptor ABCA-1 em células beta apresentam redução nas concentrações plasmáticas de insulina e são intolerantes a glicose [71]. Estes animais

apresentam diminuição em ambas primeira e segunda fase de secreção, sem redução no conteúdo total de insulina e na massa de células beta [72].

Se de um lado o aumento na concentração de colesterol interfere na secreção de insulina, por outro a lado a redução no conteúdo de colesterol também influencia no processo secretório. O bloqueio da síntese de colesterol pelo inibidor da esqualeno epoxidase, NB598, reduz o conteúdo de colesterol em aproximadamente 50%, tanto em ilhotas de camundongos quanto de humanos. Este tratamento também reduz a secreção de insulina estimulada por concentrações sub- e supra-estimulatórias de glicose [73]. Além disso, o tratamento de células com metil- β -ciclodextrina reduz a secreção de insulina por alterações na distribuição das proteínas responsáveis pela fusão do grânulo à membrana [74].

JUSTIFICATIVA

A homeostasia glicêmica depende da adequada secreção de insulina pelas células β pancreáticas assim como da ação deste hormônio nos tecidos periféricos [19, 75]. Tanto clínica quanto experimentalmente se observa uma forte relação entre distúrbios no metabolismo lipídico, obesidade induzida pela dieta, resistência à insulina e desenvolvimento de DM2 [22, 76, 77].

Resultados recentes obtidos pelo nosso grupo de pesquisa demonstraram que camundongos $LDLR^{-/-}$ alimentados com dieta padrão são intolerantes a glicose e apresentam alterações no processo de secreção de insulina [52]. As ilhotas pancreáticas destes camundongos mostram diminuição na captação de glicose, menor expressão da PKA e menor secreção de insulina frente a diferentes secretagogos [52, 78]. No entanto, outros mecanismos que levam a diminuição da secreção da insulina nas ilhotas dos $LDLR^{-/-}$ ainda precisam ser elucidados. Além disso, ainda não se dispõe de dados na literatura sobre a sinalização da insulina nos tecidos periféricos destes camundongos. Assim, decidimos avaliar neste estudo a relação entre o conteúdo de colesterol, a movimentação de cálcio e a secreção de insulina em ilhotas de camundongos $LDLR^{-/-}$. Adicionalmente, buscamos investigar a ação da insulina nos tecidos periféricos dos $LDLR^{-/-}$, assim como avaliar o efeito da dieta hiperlipídica na secreção e ação deste hormônio nestes camundongos.

OBJETIVOS

GERAL

Avaliar a relação entre o conteúdo de colesterol, movimentação de cálcio citoplasmático e secreção de insulina em ilhotas pancreáticas de camundongos $LDLR^{-/-}$. Além disso, analisar o efeito da dieta rica em gordura (HFD) sobre a homeostasia glicêmica, secreção e ação da insulina nestes camundongos.

ESPECÍFICOS

- Investigar o efeito da redução do conteúdo de colesterol, pelo tratamento das ilhotas com Metil-beta-ciclodextrina, na movimentação de cálcio intracelular e na secreção de insulina;
- Investigar os efeitos do tratamento com dieta hiperlipídica na homeostasia glicêmica e na secreção e ação da insulina nestes camundongos.

RESULTADOS

Os resultados obtidos durante a realização deste estudo estão apresentados a seguir sob a forma de dois artigos científicos:

Artigo 1- Cholesterol reduction ameliorates glucose-induced Ca^{2+} handling and insulin secretion in islets from low-density lipoprotein receptor knockout mice ($\text{LDLR}^{-/-}$) (artigo submetido)

Artigo 2- Insulin action in LDL receptor *knockout* mice ($\text{LDLR}^{-/-}$)

ARTIGO 1**CHOLESTEROL REDUCTION AMELIORATES GLUCOSE-INDUCED CALCIUM HANDLING AND INSULIN SECRETION IN ISLETS FROM LOW-DENSITY LIPOPROTEIN RECEPTOR KNOCKOUT MICE**

Souza, J. C.¹; Vanzela, E. C.¹; Ribeiro, R.A.^{1, 2}; de Oliveira, C.A.³; Carneiro, E.M.¹; Oliveira, H.C.F.¹; Boschero, A.C¹.

1 Department of Structural and Functional Institute of Biology, Stated University of Campinas (UNICAMP), Campinas, SP, Brazil.

2 Present address: Núcleo em Ecologia e Desenvolvimento Sócio-Ambiental de Macaé (NUPEM), Universidade Federal do Rio de Janeiro (UFRJ), Macaé, RJ, Brazil

3 Department of Biosciences Federal University of Sao Paulo (Unifesp), Santos, SP Brazil.

Corresponding author: Boschero, AC. Dept. of Anatomy, Cellular Biology and Physiology and Biophysics, Institute of Biology, State University of Campinas (Unicamp), Campinas, SP. P.O box 6109, Postal code 13083-970 Campinas, SP, Brazil. Tel.: +55 19 3521 6198; fax: +55 19 35216185.e-mail:boschero@unicamp.br.

Word count: Abstract 250, main text 2575

Abstract

Aims/hypothesis: Changes in cellular cholesterol levels may contribute to beta cell dysfunction. Islets from LDL receptor knockout ($\text{LDLR}^{-/-}$) possess higher cholesterol content and secrete less insulin than wild type (WT) mice. Here, we investigated the association between cholesterol content, insulin secretion and Ca^{2+} handling in these islets.

Methods: Isolated islets from both mice were used for measurements of insulin secretion (radioimmunoassay); cholesterol content (fluorimetric assay); cytosolic Ca^{2+} levels (fura-2AM) and SNARE protein expression (VAMP-2, SNAP-25 and Syntaxin-1A). Cholesterol depletion was done by incubating the islets with increasing concentrations (0-10 mmol/l) of methyl-beta-cyclodextrin (M β CD).

Results: Both first and second phase glucose-stimulated insulin secretion (GSIS) was lower in $\text{LDLR}^{-/-}$ than in WT islets, paralleled by an impairment of Ca^{2+} handling in these islets. The SNAP-25 and VAMP-2, but not Syntaxin-1A, protein contents were reduced in $\text{LDLR}^{-/-}$, compared with WT islets. Removal of the excess of cholesterol in $\text{LDLR}^{-/-}$ islets normalized glucose- and tolbutamide-induced insulin release. Glucose stimulated Ca^{2+} handling was also normalized in cholesterol-depleted $\text{LDLR}^{-/-}$ islets. Cholesterol removal from WT islets by 0.1 and 1.0 mmol/l M β CD impaired both GSIS and Ca^{2+} handling. However, 10 mmol/l M β CD markedly increased insulin secretion induced by glucose or tolbutamide in WT islets, despite a significant reduction in Ca^{2+} handling in the presence of tolbutamide.

Conclusion: Abnormal high ($\text{LDLR}^{-/-}$ islets) or low (WT islets treated with M β CD) cholesterol content alters both GSIS and Ca^{2+} handling. Normalization of cholesterol improves Ca^{2+} handling and insulin secretion in $\text{LDLR}^{-/-}$ islets, despite lowering the expression of SNAP-25 and VAMP-2 proteins.

Keywords: calcium handling, cholesterol, glucose, insulin secretion, $\text{LDLR}^{-/-}$ mice, SNARE proteins, tolbutamide

Introduction

Type 2 diabetes is a complex disease characterized by reduced insulin secretion and development of insulin resistance [79]. Frequently, diabetic patients exhibit dyslipidemia with low levels of high-density lipoprotein [31], hypertriglyceridemia [32, 33], and increased and abnormal (glycated and/or oxidized) small dense LDL particles [34]. It is known that chronic influx of fatty acids into beta cells impairs insulin secretion [80, 81]; however, emerging evidence also suggests that changes in cellular cholesterol levels may contribute to beta cell dysfunction [52, 69-71, 82].

Cholesterol constitutes about 20% of the total membrane lipids and is involved in several subcellular membrane properties such as thickness and fluidity [61, 62]. Disturbance in cholesterol metabolism results in changes in the membrane lipid raft microdomains. Numerous membrane proteins are associated with lipid rafts, including the ion channels (CaV1.2, KV2.1) [65, 66]. Additionally, SNARE proteins (Syntaxin 1A, SNAP-25, and VAMP-2) that play an essential role in the fusion of insulin-containing granules to the plasma membrane are linked to these raft microdomains in pancreatic beta cells [73, 74].

High beta cell cholesterol levels reduce the effectiveness of the insulin secretory apparatus and also interfere with glucose metabolism by inhibiting glucokinase activity [70, 83]. In the absence of a high-fat diet, islets from hypercholesterolemic $\text{LDLR}^{-/-}$ show higher cholesterol content and reduced insulin secretion in response to glucose [52]. This was associated with decreased glucose uptake and oxidation and lower expression of protein kinase A alpha [52, 78]. In this study, we investigated the involvement of Ca^{2+} handling and SNARE protein expression in the reduced insulin response in $\text{LDLR}^{-/-}$ mice islets. We also investigated the effects of cholesterol depletion in both $\text{LDLR}^{-/-}$ and WT islets and their relationship with Ca^{2+} handling and insulin secretion.

Materials and Methods

Animals

LDLR^{-/-} mice founders were purchased from the Jackson Laboratory (Bar Harbor, ME). Control wild-type (WT) mice (C57BL/6 background) were obtained from the breeding colony of the State University of Campinas (UNICAMP). Animal experiments were approved by the University's Committee for Ethics in Animal Experimentation (CEUA/UNICAMP). The mice

had free access to standard laboratory rodent chow diet (Nuvital CR1, Colombo, PR, Brazil) and water *ad libitum* and were housed at 22 ± 1°C on a 12 h light/dark cycle.

Pancreatic islet isolation and static insulin secretion

The pancreatic islets were isolated from fed mice (20 week-old) by collagenase digestion and then selected with a microscope to exclude any contaminating tissues [84]. After isolation, batches of 4 islets from each group were pre-incubated in Krebs-Ringer bicarbonate buffer (KRBB) containing, in mmol/l: 115 NaCl, 5 KCl, 24 NaHCO₃, 2.56 CaCl₂, 1 MgCl₂ and 25 HEPES, pH 7.4 plus 2.8 mmol/l glucose and 0.3% bovine serum albumin (BSA) for 30 min at 37°C. The islets were further incubated for 1 h in KRBB containing glucose (2.8 or 11.1 mmol/l) or tolbutamide 100 µmol/l. Aliquots of the supernatant at the end of the incubation period were kept at -20°C for posterior insulin measurement by RIA [85].

Perfusion studies

Groups of 50 islets from WT and LDLR^{-/-} mice were placed on a Millipore SW 1300 filter (8 µm pore) in a perfusion chamber (four chambers for each perfusion) and perfused in a KRBB buffer for 100 min at a flow rate of 1 ml/min. Glucose (2.8 mmol/l) was present from the onset of the experiment and was elevated to 11.1 mmol/l glucose from the 60th min onward. Solutions were gassed with 95% O₂/5% CO₂ and maintained at 37°C. Insulin released into the medium was measured by RIA [20].

Islet cholesterol measurement and depletion

Cholesterol content was quantified by a fluorometric method using an enzyme-coupled reaction provided by the Amplex Red Cholesterol Assay kit (Molecular Probes), as previously described [70]. Lipid extraction from groups of 10 islets per mice of each group were performed with chloroform/methanol (2:1 vol/vol), dried down under a N₂ stream, and diluted in 60 µl of working solution (Amplex Red Cholesterol Assay kit) supplemented with 0.1% Triton X- 100. Of this sample, 50 µl were used for the cholesterol assay. For cholesterol depletion, islets were pre-incubated with 0.1, 1 or 10 mmol/l of methyl-β-cyclodextrin (MβCD) (Sigma-Aldrich) at 37°C for 1 h. Islets were then washed in KRBB (5.6 mmol/l) and used in the experiments.

Cytoplasmatic Ca²⁺ Oscillations

Fresh pancreatic islets were incubated in KRBB plus 5.6 mmol/l glucose and 5 µmol/l Fura-2/AM for 1 h at 37°C. Islets previously incubated with MβCD were washed three times with KRBB and incubated with Fura-2/AM, as described above. Islets were then transferred to a thermostatically-regulated open chamber (37°C), placed on the stage of an inverted microscope (Nikon UK, Kingston, UK), and perfused with KRBB at a flow rate of 1.5 ml/min. Islets were then perfused with KRBB continuously gassed with 95% O₂/5% CO₂, pH 7.4 containing 2.8 mmol/l with or without 100µmol/l tolbutamide or 11.1 mmol/l glucose. A ratio image was acquired at approximately every 5s with an ORCA-100 CCD camera (Hammamatsu Photonics Iberica, Barcelona, Spain), in conjunction with a Lambda-10- CS dual filter wheel (Sutter Instrument Company, CA, USA), equipped with 340 and 380 nm, 10 nm bandpass filters and a range of neutral density filters (Omega opticals, Stanmore, UK). Data were obtained using the ImageMaster3 software (Photon Technology International, NJ, USA). The area under the curve was calculated during the period that the stimulus was present in the medium, after subtracting the basal values (2.8 mmol/l glucose).

Western blotting

Isolated islets from LDLR^{-/-} and WT mice were homogenized in a buffer containing (in mmol/l): 100 Tris pH 7.5, 10 sodium pyrophosphate, 100 sodium fluoride, 10 EDTA, 10 sodium vanadate, 2 PMSF and 1% Triton-X 100). The islets were disrupted using a Polytron

PT 1200 C homogenizer (Brinkmann Instruments, NY, USA), employing three 10s pulses. The extracts were then centrifuged at 12,600g at 4°C for 5 min to remove insoluble material. The protein concentration in the supernatants was assayed using the Bradford dye method [86], using BSA as a standard curve and Bradford reagent (Bio-Agency Lab., São Paulo, SP, BRA). For SDS gel electrophoresis and Western blot analysis, the samples were treated with a Laemmli sample buffer containing dithiothreitol. After heating to 95°C for 5 min, the proteins were separated by electrophoresis (50 µg protein/lane, 8% gels) and, afterwards, transferred to nitrocellulose membranes. The nitrocellulose filters were treated overnight with a blocking buffer (5% non-fatdried milk, 10 mmol/l Tris, 150 mmol/l NaCl, and 0.02% Tween 20) and were subsequently incubated with an antibody against SNAP-25 [S-5187; mouse monoclonal; Sigma (St. Louis, MO)], VAMP-2 [627724; rabbit polyclonal; Calbiochem (La Jolla, CA)], Syntaxin-1A[sc-12736; mouse monoclonal; Santa Cruz Biotechnology (Santa Cruz, CA)]. Specific protein bands were visualized by incubating the membranes for 1 h with a peroxidase-conjugated secondary antibody (1:10.000; Zymed Laboratories, Inc., San Francisco, CA, USA), followed by detection with enhanced 151 chemiluminescence reagents (Pierce Biotechnology, USA) and exposure to X-ray film (Kodak, AM, Brazil). The band intensities were quantified by optical densitometry (Un-Scan-It gel, version 6.1, Orem, Utah, USA). After assaying the target proteins, Western blotting was repeated using rabbit polyclonal antibody to GAPDH [1:1.000; cat. (FL-335): sc-25778], used as an internal control for proteins.

Statistical analysis

Results are presented as means ± SEM for the number of determinations (n) indicated. The data were analyzed by unpaired Student's t-test for two mean comparisons and two-way ANOVA (with Neuman–Keuls post-hoc test) for dose–response experiments. The level of significance was set at p<0.05 and analyses were performed using Statistica version 7.0 for Windows (Stat Soft Inc, Tulsa, OK, USA).

Results

Glucose-stimulated insulin release and [Ca²⁺]i rise were reduced in LDLR^{-/-} islets

As previously reported [52], LDLR^{-/-} release less insulin in both the first and second phase, when compared with WT mice ($p < 0.05$) (Fig.1). Since the increase in [Ca²⁺]i is a key step in insulin secretion, we examined the glucose-stimulated Ca²⁺ handling in islets from LDLR^{-/-}. A representative example of the Ca²⁺ response is shown in Figure 2 (A). Elevation of glucose from 2.8 to 11.1 mmol/l induced a [Ca²⁺]i rise in both groups; however, the amplitude of oscillations was significantly smaller in LDLR^{-/-} than WT islets. As shown in Figure 2 (B), the area under the curve (AUC) of the glucose-evoked [Ca²⁺]i rise was significantly reduced in the islets of LDLR^{-/-} mice. During the first 6 min of exposure to high glucose (first phase release) as well as between min 6 and 20 (second phase release), the AUCs of glucose-evoked [Ca²⁺]i rise were significantly diminished in LDLR^{-/-} islets (D). The insulin secretion in the presence of tolbutamide was also markedly reduced in LDLR^{-/-} islets (1.22 ± 0.16 vs. 0.50 ± 0.11 , respectively; $p < 0.05$). Accordingly, the AUC of the tolbutamide-evoked [Ca²⁺]i rise was also reduced in LDLR^{-/-} islets (Fig 3 A-B).

Reduced expression of SNARE proteins in LDLR^{-/-}

Insulin granule exocytosis is a multiple-step process that depends upon the elevation of [Ca²⁺]i. Since the alterations in Ca²⁺ handling induced by glucose and tolbutamide were attenuated in LDLR^{-/-}, compared with WT islets, especially during the second phase release (Fig 1D), it is conceivable that the exocytic process could also be hampered in the former islets. In fact, the expressions of SNAP-25 and VAMP-2, but not Syntaxin-1A, were reduced by 30% in LDLR^{-/-}, compared with WT islets ($p < 0.05$) (Fig 4).

Reduction in the intra-islet cholesterol ameliorates the glucose-stimulated Ca²⁺ rise and insulin secretion in LDLR^{-/-} mice

We have previously shown that cholesterol content is higher in LDLR^{-/-} than in WT islets [11]. Therefore, we analyzed whether the reduction of islet cholesterol content modifies Ca²⁺ handling. For this purpose, islets from both groups were previously treated with MβCD.

Cholesterol content in $\text{LDLR}^{-/-}$ islets, treated with 0.1 mmol/l M β CD, was reduced to similar levels found in WT islets (Fig 5), and M β CD-treated WT islets showed a marginal decrease in cholesterol content. Figure 6 shows that treatment reduced glucose-induced Ca^{2+} oscillations in WT islets. The $[\text{Ca}^{2+}]_i$ AUC of M β CD treated islets were diminished compared WT islets. Glucose-induced $[\text{Ca}^{2+}]_i$ modifications in islets from $\text{LDLR}^{-/-}$ treated with increasing concentrations of M β CD showed a different behavior when compared with WT islets (Fig 6). In these islets, the $[\text{Ca}^{2+}]_i$ AUC were progressively augmented with increasing M β CD concentrations. At 0.1 and 1.0 mmol/l M β CD, the $[\text{Ca}^{2+}]_i$ rise resulted in levels similar to those observed in WT islets without M β CD. At 10 mmol/l M β CD, the AUC was significantly higher (2-fold) than $\text{LDLR}^{-/-}$ islets without M β CD (Fig 6C).

We also examined the relationship between islet cholesterol content and beta cell function. For this purpose, glucose-stimulated insulin secretion was measured in islets from WT and $\text{LDLR}^{-/-}$ treated with different concentrations of M β CD. Glucose-induced insulin secretion was increased with increasing concentrations of M β CD only in $\text{LDLR}^{-/-}$ islets (Fig 7). In WT islets, there was a significant reduction in glucose-stimulated insulin secretion at 1.0 mmol/l, but a marked increase at 10 mmol/l M β CD.

A significant increase in tolbutamide-stimulated insulin release was also observed in WT islets treated with 10 mmol/l M β CD (Fig 9). In addition, 10 mmol/l M β CD significantly decreased the AUC of the tolbutamide-induced $[\text{Ca}^{2+}]_i$ rise in WT islets (Fig 8). In $\text{LDLR}^{-/-}$, tolbutamide-induced insulin secretion (Fig 9), but not $[\text{Ca}^{2+}]_i$ (Fig 8), was increased, although to a lesser extent than in WT islets.

Discussion

It has been recently shown that cholesterol content in $\text{LDLR}^{-/-}$ is higher than in WT islets [52]. Since glucose-induced insulin secretion is lower in $\text{LDLR}^{-/-}$, we investigated the relationship between cholesterol content, insulin secretion and Ca^{2+} handling in these islets. Higher cholesterol content is associated with a decrease in fluidity [87], as well as an increase in the stiffness [88] of the membrane, and these alterations may cause an inappropriate distribution or functioning of membrane proteins. In this respect, alterations in the distribution and activity of ion channels and modifications of the distribution of SNARE proteins, linked to cholesterol clusters in the membrane, were previously observed in pancreatic beta cells [64, 89]. In addition, increased islet cholesterol levels by selective deletion of ABCA1 gene in apoE knockout mice resulted in reduced glucose-stimulated insulin secretion [90]. Furthermore, INS-1 cells overloaded with cholesterol secrete less insulin in response to glucose, possibly due to a reduction in glucokinase activity [70] that, ultimately, reflects alterations in membrane depolarization [91]. Here, we observed that glucose- and tolbutamide-induced insulin secretion as well as Ca^{2+} handling in $\text{LDLR}^{-/-}$ was lower than in WT islets (Figs. 1, 2, 3 and 5). Moreover, SNAP-25 and VAMP-2 expressions were also reduced in $\text{LDLR}^{-/-}$. The lower expressions of these two proteins, which participate in the traffic of insulin-containing vesicles, could explain the lower insulin secretion observed during the second phase release in $\text{LDLR}^{-/-}$ islets. Cellular cholesterol also influences the trafficking of proteins from cytosolic to membrane rafts microdomains [67] and is important in coordinating the assembly of calcium channels with SNARE proteins during the exocytotic process [68, 73]. Thus, the excess of cholesterol observed in islets from $\text{LDLR}^{-/-}$ may be responsible for the impairment of Ca^{2+} handling and insulin secretion.

While results from the literature indicate that high levels of cellular cholesterol impair glucose-induced insulin secretion, information concerning the reduction of cellular cholesterol is contradictory [66, 70, 73, 91]. Here, we confirm that removal of the excess of cholesterol from islets of $\text{LDLR}^{-/-}$ by increasing concentrations of M β CD improved glucose-induced insulin secretion and that this improvement is linked to a better Ca^{2+} handling by these islets. Recently, it was demonstrated that cholesterol-enriched mouse beta cells show a lower voltage gated calcium channel (VGCC) density, which diminishes Ca^{2+} influx and, in turn, triggers a lower insulin secretion. Since, in the presence of M β CD, tolbutamide increased insulin

secretion, but did not modify the Ca^{2+} signal in $\text{LDLR}^{-/-}$ islets, cholesterol normalization could improve components of the Ca^{2+} -induced release process, other than VGCC density (not addressed in this study).

In contrast to observations in $\text{LDLR}^{-/-}$, when cholesterol was removed from WT islets with low concentrations of M β CD (0.1 and 1 mmol/l), the glucose-induced $[\text{Ca}^{2+}]_i$ increase was lower and insulin secretion was significantly reduced. However, at 10 mmol/l M β CD, a significant increase in insulin secretion was noticed, while $[\text{Ca}^{2+}]_i$ was lower than in WT without M β CD. Furthermore, in WT islets, the tolbutamide-induced Ca^{2+} signal was also lowered by 10 mmol/l M β CD, whereas insulin secretion was increased. Reduction of cholesterol levels in rodent islets with a squalene epoxidase inhibitor (NB598) reduced insulin secretion, whole-cell delayed Ca^{2+} currents, and granule mobilization. In MIN6 cells, NB598 also provoked a redistribution of membrane proteins such as Kv2.1, Cav1.2, syntaxin-1A, SNAP-25, and VAMP [73]. We hypothesize that, in the presence of lower concentrations of M β CD, several of the above-mentioned alterations obtained with NB598 may occur in our experiments, thus justifying the lower Ca^{2+} handling and insulin secretion. However, the marked increase in insulin secretion induced by tolbutamide with low Ca^{2+} , in the presence of 10 mmol/l M β CD, is more difficult to explain. It may be postulated that excessive removal of cholesterol from the membrane is toxic and provoke insulin release from damaged cells by a Ca^{2+} -independent mechanism.

In conclusion, the ability of glucose-induced insulin secretion, as well as Ca^{2+} handling, are impaired in $\text{LDLR}^{-/-}$, compared with WT islets. In addition, the SNAP-25 and VAMP-2, but not Syntaxin-1A, protein contents were also reduced in $\text{LDLR}^{-/-}$ islets. An adequate reduction in the excess of cholesterol normalized insulin secretion and Ca^{2+} handling. However, a decrease in cholesterol in WT islets impaired Ca^{2+} handling and insulin secretion. These data indicate that both excess and deficiency of cholesterol concentration in islets alter glucose-induced Ca^{2+} oscillations and, consequently, insulin secretion.

Acknowledgements: This study was supported by the Brazilian foundations: Fundação de Amparo à Pesquisa do Estado de São Paulo, Coordenação de Aperfeiçoamento de Pessoal de Nível Superior, Conselho Nacional de Pesquisa and Instituto Nacional de Ciência e Tecnologia de Obesidade e Diabetes. We thank Mr. L. Domingos for technical assistance and Nicola Conran for editing English.

Author contributions: Souza, JC: conception and experimental design, execution of all experiments, analyses, data interpretation, and manuscript writing; Vanzela EC experimental execution and intellectual contribution during work development; Ribeiro, RA: design and execution of insulin secretion experiments; de Oliveira, CA execution of calcium experiments; Carneiro, EM: intellectual contribution during work development; Oliveira HCF and Boschero AC: conception and experimental design, data interpretation, manuscript writing and reviewing the final version of paper.

Duality of interest: The authors declare that there is no duality of interest associated with this manuscript

References

- [1] Perley MJ, Kipnis DM (1967) Plasma insulin responses to oral and intravenous glucose: studies in normal and diabetic subjects. *J Clin Invest* 46: 1954-1962.
- [2] Ginsberg HN (1996) Diabetic dyslipidemia: basic mechanisms underlying the common hypertriglyceridemia and low HDL cholesterol levels. *Diabetes* 45 Suppl 3: S27-30.
- [3] Wilson PW, McGee DL, Kannel WB (1981) Obesity, very low density lipoproteins, and glucose intolerance over fourteen years: The Framingham Study. *Am J Epidemiol* 114: 697-704.
- [4] Lewis GF, Carpentier A, Adeli K, Giacca A (2002) Disordered fat storage and mobilization in the pathogenesis of insulin resistance and type 2 diabetes. *Endocr Rev* 23: 201-229.
- [5] Reaven GM, Chen YD, Jeppesen J, Maheux P, Krauss RM (1993) Insulin resistance and hyperinsulinemia in individuals with small, dense low density lipoprotein particles. *J Clin Invest* 92: 141-146.
- [6] Cerf ME (2007) High fat diet modulation of glucose sensing in the beta-cell. *Med Sci Monit* 13: RA12-17.
- [7] Eto K, Yamashita T, Matsui J, Terauchi Y, Noda M, Kadokawa T (2002) Genetic manipulations of fatty acid metabolism in beta-cells are associated with dysregulated insulin secretion. *Diabetes* 51 Suppl 3: S414-420.
- [8] Hao M, Head WS, Gunawardana SC, Hasty AH, Piston DW (2007) Direct effect of cholesterol on insulin secretion: a novel mechanism for pancreatic beta-cell dysfunction. *Diabetes* 56: 2328-2338.
- [9] Brunham LR, Kruit JK, Pape TD, et al. (2007) Beta-cell ABCA1 influences insulin secretion, glucose homeostasis and response to thiazolidinedione treatment. *Nat Med* 13: 340-347.
- [10] Ishikawa M, Iwasaki Y, Yatoh S, et al. (2008) Cholesterol accumulation and diabetes in pancreatic beta-cell-specific SREBP-2 transgenic mice: a new model for lipotoxicity. *J Lipid Res* 49: 2524-2534.
- [11] Bonfleur ML, Vanzela EC, Ribeiro RA, et al. (2010) Primary hypercholesterolaemia impairs glucose homeostasis and insulin secretion in low-density lipoprotein receptor knockout mice independently of high-fat diet and obesity. *Biochim Biophys Acta* 1801: 183-190.

- [12] de Souza JC, de Oliveira CA, Carneiro EM, Boschero AC, de Oliveira HC (2010) Cholesterol toxicity in pancreatic islets from LDL receptor-deficient mice. *Diabetologia* 53: 2461-2462; author reply 2463-2464.
- [13] Ohvo-Rekilä H, Ramstedt B, Leppimäki P, Slotte JP (2002) Cholesterol interactions with phospholipids in membranes. *Prog Lipid Res* 41: 66-97.
- [14] Rög T, Pasenkiewicz-Gierula M (2003) Effects of epicholesterol on the phosphatidylcholine bilayer: a molecular simulation study. *Biophys J* 84: 1818-1826.
- [15] Wiser O, Trus M, Hernández A, et al. (1999) The voltage sensitive Lc-type Ca²⁺ channel is functionally coupled to the exocytotic machinery. *Proc Natl Acad Sci U S A* 96: 248-253.
- [16] Xia F, Gao X, Kwan E, et al. (2004) Disruption of pancreatic beta-cell lipid rafts modifies Kv2.1 channel gating and insulin exocytosis. *J Biol Chem* 279: 24685-24691.
- [17] Vikman J, Jimenez-Feltström J, Nyman P, Thelin J, Eliasson L (2009) Insulin secretion is highly sensitive to desorption of plasma membrane cholesterol. *FASEB J* 23: 58-67.
- [18] Xia F, Xie L, Mihic A, et al. (2008) Inhibition of cholesterol biosynthesis impairs insulin secretion and voltage-gated calcium channel function in pancreatic beta-cells. *Endocrinology* 149: 5136-5145.
- [19] Rizzo MA, Magnuson MA, Drain PF, Piston DW (2002) A functional link between glucokinase binding to insulin granules and conformational alterations in response to glucose and insulin. *J Biol Chem* 277: 34168-34175.
- [20] Bonfleur ML, Ribeiro RA, Balbo SL, et al. (2011) Lower expression of PKAα impairs insulin secretion in islets isolated from low-density lipoprotein receptor (LDLR(-/-)) knockout mice. *Metabolism* 60: 1158-1164.
- [21] Boschero AC, Delattre E (1985) The mechanism of gentamicin-inhibited insulin release by isolated islets. *Arch Int Pharmacodyn Ther* 273: 167-176.
- [22] Scott AM, Atwater I, Rojas E (1981) A method for the simultaneous measurement of insulin release and B cell membrane potential in single mouse islets of Langerhans. *Diabetologia* 21: 470-475.
- [23] Bradford MM (1976) A rapid and sensitive method for the quantitation of microgram quantities of protein utilizing the principle of protein-dye binding. *Anal Biochem* 72: 248-254.
- [24] Colell A, García-Ruiz C, Lluis JM, Coll O, Mari M, Fernández-Checa JC (2003) Cholesterol impairs the adenine nucleotide translocator-mediated mitochondrial permeability transition through altered membrane fluidity. *J Biol Chem* 278: 33928-33935.

- [25] Lundbaek JA, Birn P, Girshman J, Hansen AJ, Andersen OS (1996) Membrane stiffness and channel function. *Biochemistry* 35: 3825-3830.
- [26] Churchward MA, Rogasevskaia T, Höfgen J, Bau J, Coorssen JR (2005) Cholesterol facilitates the native mechanism of Ca²⁺-triggered membrane fusion. *J Cell Sci* 118: 4833-4848.
- [27] Takahashi N, Hatakeyama H, Okado H, et al. (2004) Sequential exocytosis of insulin granules is associated with redistribution of SNAP25. *J Cell Biol* 165: 255-262.
- [28] Kruit JK, Kremer PH, Dai L, et al. (2010) Cholesterol efflux via ATP-binding cassette transporter A1 (ABCA1) and cholesterol uptake via the LDL receptor influences cholesterol-induced impairment of beta cell function in mice. *Diabetologia* 53: 1110-1119.
- [29] Hao M, Bogan JS (2009) Cholesterol regulates glucose-stimulated insulin secretion through phosphatidylinositol 4,5-bisphosphate. *J Biol Chem* 284: 29489-29498.
- [30] Lang T, Bruns D, Wenzel D, et al. (2001) SNAREs are concentrated in cholesterol-dependent clusters that define docking and fusion sites for exocytosis. *EMBO J* 20: 2202-2213.
- [31] Ohara-Imaiizumi M, Nishiwaki C, Nakamichi Y, Kikuta T, Nagai S, Nagamatsu S (2004) Correlation of syntaxin-1 and SNAP-25 clusters with docking and fusion of insulin granules analysed by total internal reflection fluorescence microscopy. *Diabetologia* 47: 2200-2207.

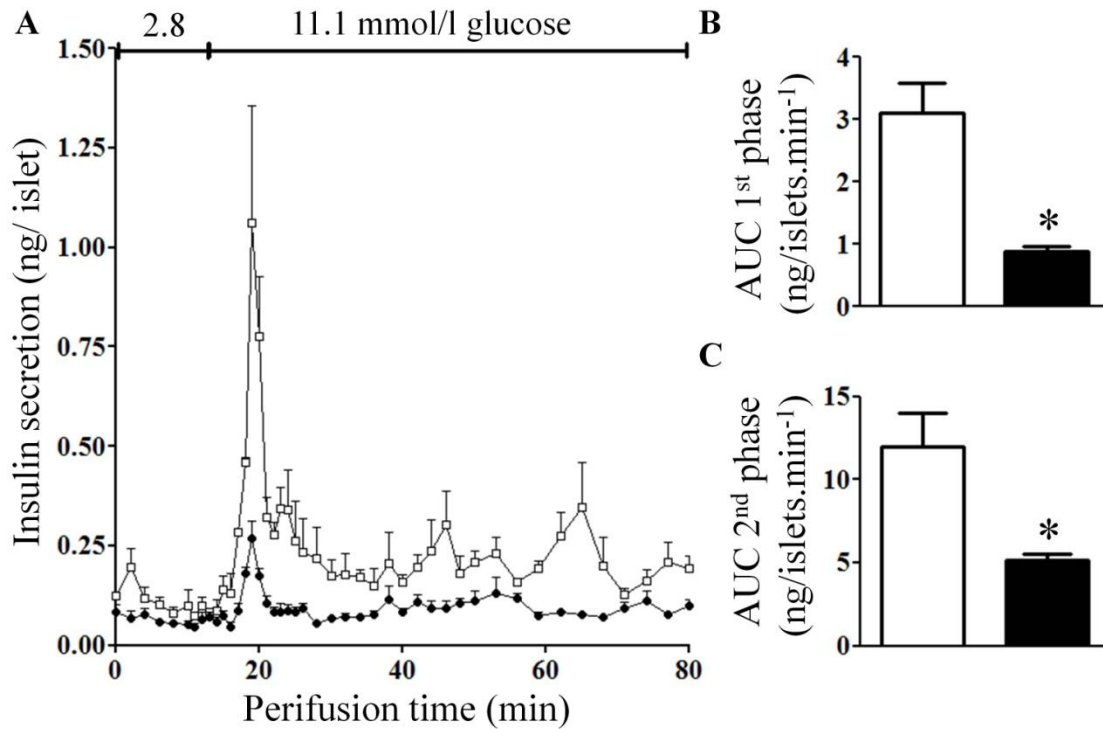
FIGURES

Fig.1. Effects of 11.1 mmol/l glucose on the dynamics of insulin release from WT (open squares and open bars) and LDLR^{-/-} (solid circles and dark bars) mice islets. Groups of 50 freshly isolated islets were perfused for 80 min (A). Glucose at 2.8 mmol/l was present from the onset of the experiment and was increased to 11.1 mmol/l from min 16 until the end of the perfusion period. Cumulative insulin release during the first phase (B), measured as AUC1 between time points $t=16$ and 22 min, and summed insulin release during the second phase (AUC2), measured between time points $t=23$ and 80 min (C). Values are means \pm SEM of four distinct experiments. * $p<0.05$ vs. WT.

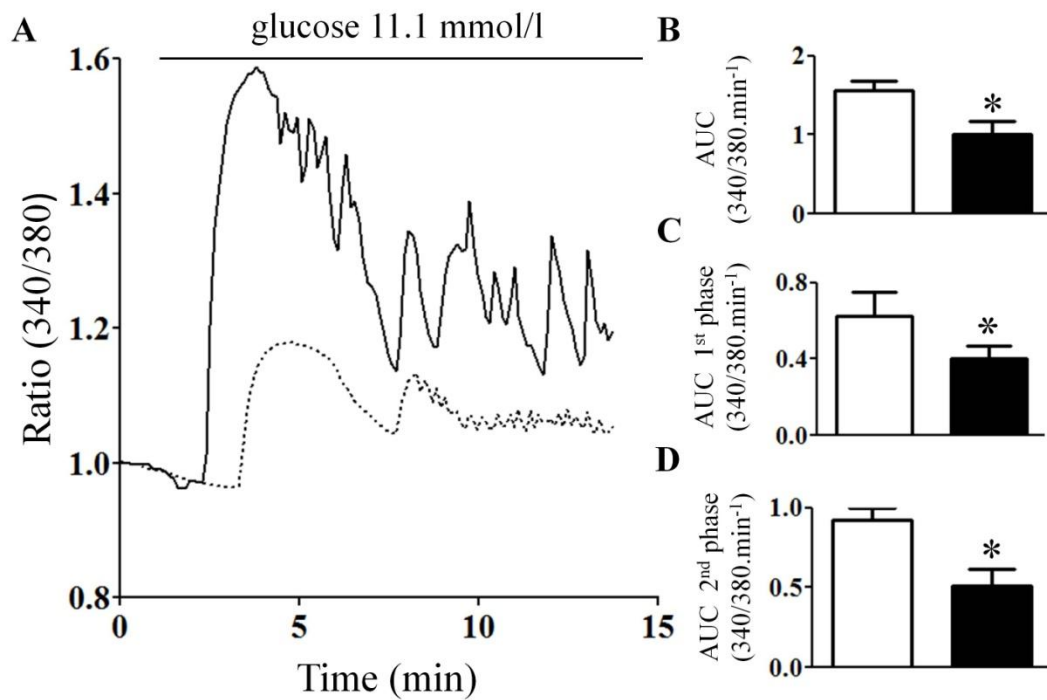


Fig. 2. Representative curves of changes in intracellular Ca^{2+} concentrations in response to 11.1 mmol/l glucose in WT (solid line and open bars) and $\text{LDLR}^{-/-}$ (dotted lines and dark bars) mice islets (A). The Area Under the Curves (AUC) was calculated for 3 different periods at 11.1 mmol/l glucose: B (1-15 min), C (1-6 min), and D 6-15 min of perfusion. Values are the ratios of F340/F380 registered for each group. Data are means \pm SEM of 4 independent experiments. * $p<0.05$ indicates significant difference vs WT.

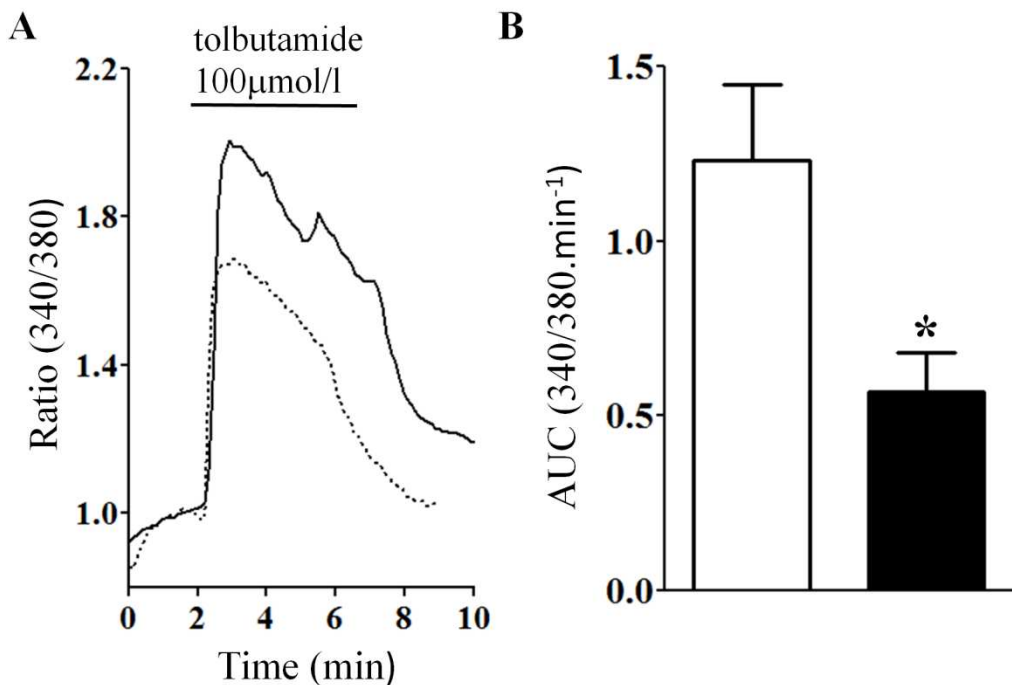


Fig. 3 – Tolbutamide (100 $\mu\text{mol/l}$) induced Ca^{2+} rise in WT (solid line and open bar) and $\text{LDLR}^{-/-}$ (dotted line and dark bar) mice islets (A). The Area Under the Curves (AUC) was calculated when tolbutamide was present in the perfusion period (B). Values are the ratios of F340/F380 registered for each group. Data are means \pm SEM from 7 independent experiments. * $p<0.05$ indicates significant difference vs WT.

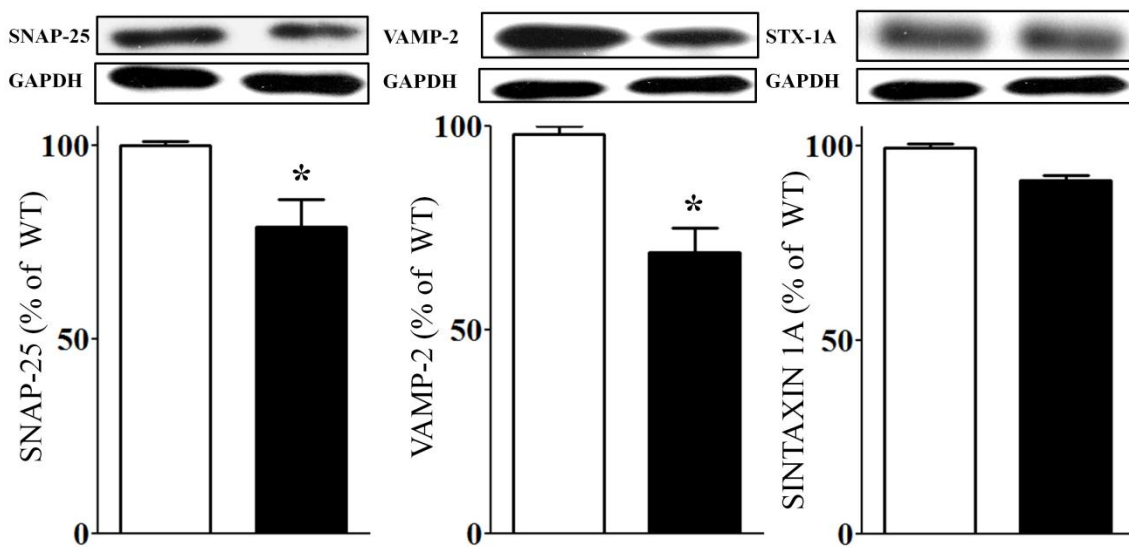


Fig. 4 – SNAP-25 (A), VAMP-2 (B) and Syntaxin-1A (C), protein expression in isolated islets from WT (open bars) and Ldlr^{-/-} (dark bars) mice. Protein extracts were processed for Western blotting. The bars represent the means \pm SEM of the values, determined by optical densitometry. n = (3-5). *p<0.05 vs WT.

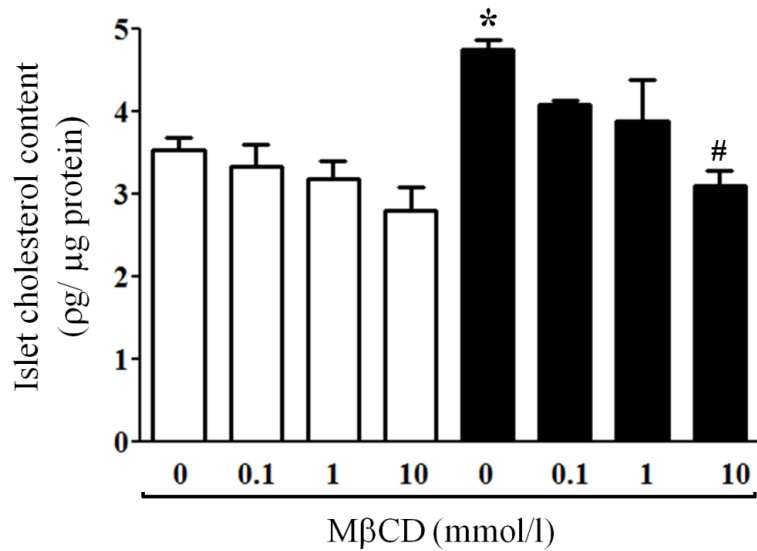


Fig. 5 Cholesterol levels from WT (open bars) and $\text{LDLR}^{-/-}$ (dark bars) mice islets. Cholesterol depletion was done by incubating the islets in the presence of increasing concentrations of M β CD for 1 h at 37°C. Values represent means \pm SEM * $p<0.05$ compared WT (without M β CD); # $p<0.05$ compared $\text{LDLR}^{-/-}$ (without M β CD).

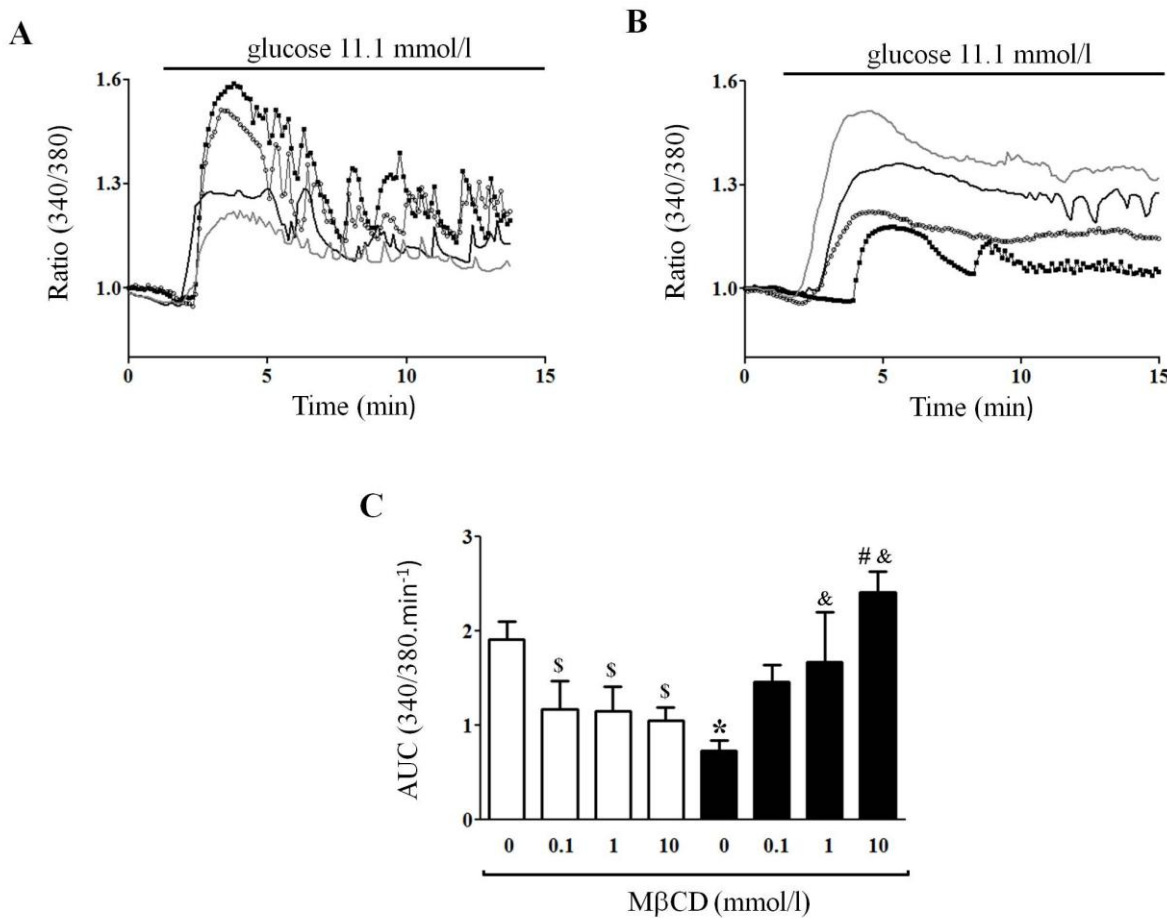


Fig. 6 Effects of M β CD treatment on glucose induced [Ca₂₊]i rise in WT and LDLR-/- mice islets. (A) Representative curves of changes in intracellular Ca₂₊ concentrations in response to 11.1 mmol/l glucose in WT islets; WT (line with solid squares), WT+0.1mmol/l M β CD (line with open circles), WT+1mmol/l M β CD (dotted line), and WT+10mmol/l M β CD (solid line). (B) Representative curves of changes in intracellular Ca₂₊ concentrations in response to 11.1 mmol/l glucose in LDLR-/- islets; LDLR-/- (line with solid squares), LDLR-/-+0.1mmol/l M β CD (line with open circles), LDLR-/- +1mmol/l M β CD (dotted line), and LDLR-/- +10mmol/l M β CD (solid line). (C) AUC from glucose induced calcium rise. Values are the ratios of F340/F380 registered for each group. Data are means \pm SEM for 4-9 independent experiments. * P < 0.05 compared WT (without M β CD); # P < 0.05 compared LDLR-/- (without M β CD); \$ P < 0.05 compared WT (without M β CD) by one-way ANOVA; & < 0.05 compared LDLR-/- (without M β CD) by one-way ANOVA.

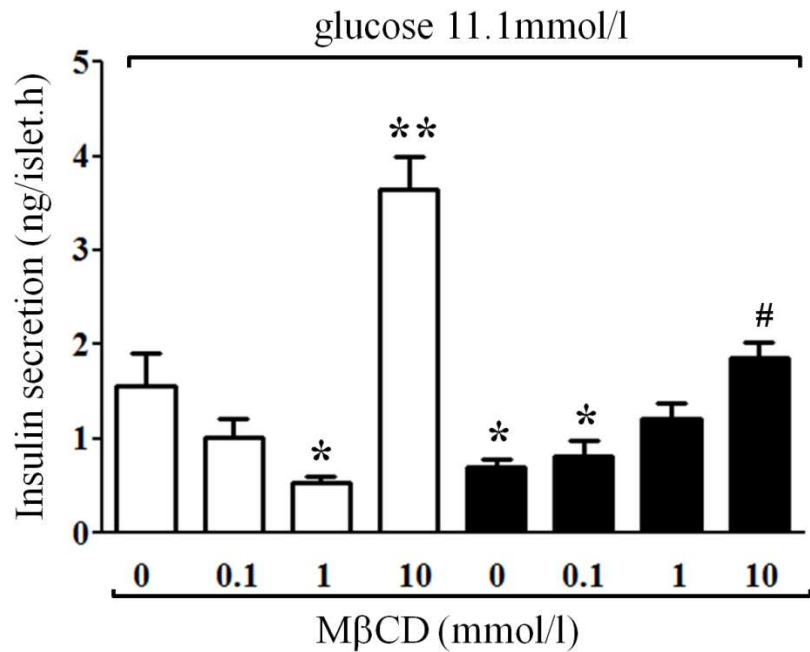


Fig. 7 Effects of cholesterol depletion on the glucose-induced insulin secretion by WT (open bars) and $\text{LDLR}^{-/-}$ (dark bars) mice islets. Cholesterol depletion was done by incubating the islets in the presence of increasing concentrations of M β CD for 1 h at 37°C. Each bar represents mean \pm SEM of 12-20 groups of islets from 6 different mice. * $p<0.05$ vs. WT; ** $p<0.01$ vs WT; # $p<0.05$, vs $\text{LDLR}^{-/-}$.

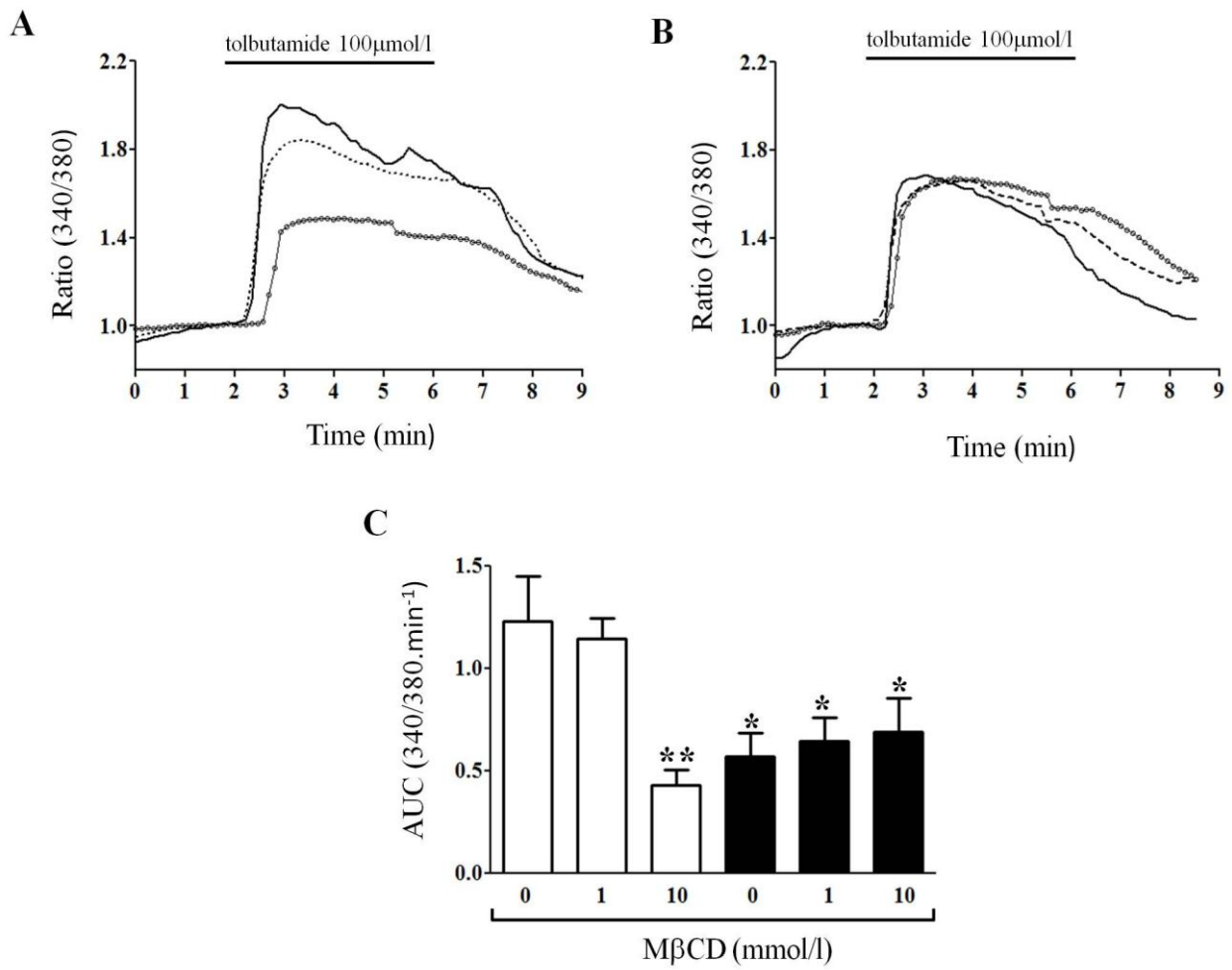


Fig. 8 Effects of M β CD treatment on tolbutamide-induced $[Ca^{2+}]_i$ rise in WT and LDLR $^{-/-}$ mice islets. (A) Representative curves of changes in intracellular Ca^{2+} concentrations in response to tolbutamide in WT islets; WT (solid line), WT+1mmol/l M β CD (dotted line), and WT+10mmol/l M β CD (line with open circles), and LDLR $^{-/-}$ islets (B): LDLR $^{-/-}$ (solid line), LDLR $^{-/-}$ +1mmol/l M β CD (dotted line), and LDLR $^{-/-}$ +10mmol/l M β CD (line with open circles). (C) Area under de curve (AUC) from tolbutamide induced calcium rise. Values are the ratios of F340/F380 registered for each group. Data are means \pm SEM from 5-7 independent experiments. *p<0.05 vs WT (without M β CD); **p<0.01 vs WT (without M β CD); # p<0.05 compared LDLR $^{-/-}$ (without M β CD).

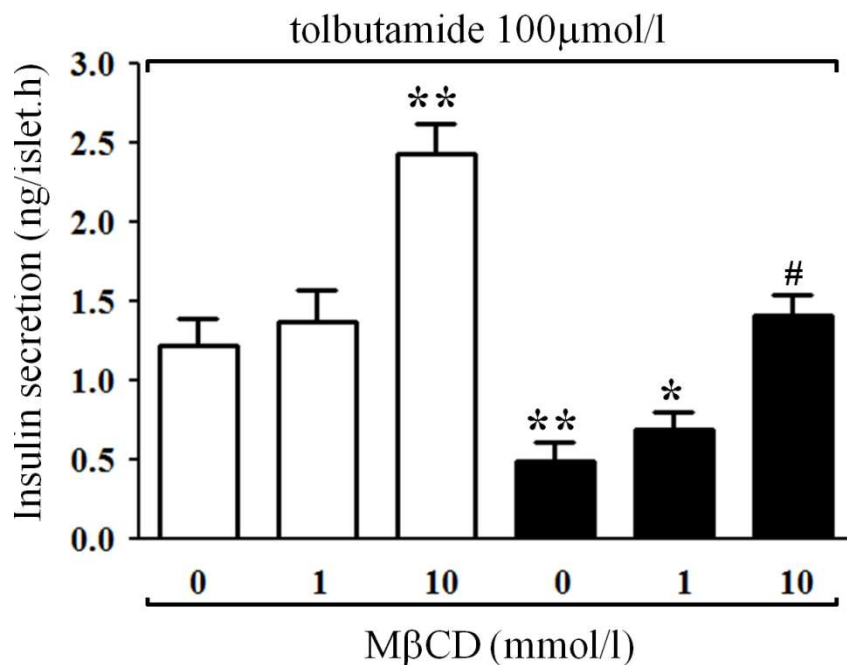


Fig. 9 – Effects of cholesterol depletion on the tolbutamide-induced insulin secretion in WT (open bars) and LDLR^{-/-} (dark bars) mice islets. Cholesterol depletion was done by incubating the islets in the presence of increasing concentrations of MβCD for 1 h at 37°C. Each bar represents mean ± SEM of 10-16 groups of islets from 6 different mice. *p<0.05 vs. WT (without MβCD); **p<0.01 vs WT (without MβCD); #p<0.05, vs LDLR^{-/-} (without MβCD).

ARTIGO 2:**INSULIN ACTION IN LDL RECEPTOR *KNOCKOUT* MICE (LDLR^{-/-}) FED LOW OR HIGH-FAT DIET**

Souza, J. C.¹; Vanzela, E. C.¹; Ribeiro, R.A.^{1,2}; Rezende, L.F.¹; Carneiro, E.M.¹; Oliveira, H.C.F.¹; Boschero, A.C¹.

1 Department of Structural and Functional Biology. Institute of Biology, Stated University of Campinas (UNICAMP), Campinas, SP, Brazil.

2 Present address: Núcleo em Ecologia e Desenvolvimento Sócio-Ambiental de Macaé (NUPEM), Universidade Federal do Rio de Janeiro (UFRJ), Macaé, RJ, Brazil

Corresponding author: Boschero, AC. Dept. of Structural and Functional Biology, Institute of Biology, State University of Campinas (Unicamp), Campinas, SP. P.O box 6109, Postal code 13083-970 Campinas, SP, Brazil. Tel.: +55 19 3521 6198; fax: +55 19 35216185.
e-mail:boschero@unicamp.br.

Abstract

Aims/hypothesis: Changes in body fat mass and in serum lipids are associated with the development of insulin resistance. Here, we investigated the insulin signaling in liver, muscle and adipose tissue of $\text{LDLR}^{-/-}$ mice, fed a chow or a high-fat diet (HFD).

Methods: Male $\text{LDLR}^{-/-}$ and wild-type (WT) mice, 4 months of age, were fed with HFD (western-type, 40% Kcal by fat) or a chow-diet for 30 days. Glucose homeostasis was analyzed using oral glucose tolerance test (oGTT) (1.5 g/ Kg body weight); total cholesterol (CHOL), triglycerides (TG), non-esterified fatty acids (NEFA) and plasma insulin by standard commercial kits; Insulin secretion by isolated islets, by RIA; Insulin signaling by immunoprecipitation and immunoblotting of $\text{IR}\beta$ and pAKT and Insulin Degrading Enzyme (IDE) expression by western-blot.

Results: $\text{LDLR}^{-/-}$ showed high plasma levels of CHOL, TG, glucose and increased mass of epididymal fat depot compared with WT. These mice were glucose intolerants but more sensitive to insulin than WT, especially in muscle and liver. The IDE protein expression was lower in $\text{LDLR}^{-/-}$ than in WT mice. HFD promoted a higher body weight gain and worsened the glucose tolerance and insulin signaling $\text{LDLR}^{-/-}$ mice. In WTH mice HFD induced an increase in plasma insulin levels while the insulin signaling was only altered in muscle.

Conclusion: The results indicate that $\text{LDLR}^{-/-}$ mice fed a chow diet are more sensitive to insulin probably due to adaptive mechanisms that compensate lower insulin secretion. However, these changes are not sufficient to maintain glucose homeostasis since these mice were glucose intolerants. When fed a high-fat diet, they became also insulin resistant probably due to an increase in visceral adipose tissue mass.

Keywords: High-fat diet, Insulin Degrading Enzyme (IDE), insulin resistance, insulin signaling, $\text{LDLR}^{-/-}$ mice.

Introduction

Type 2 diabetes mellitus is a complex metabolic disease which onset and development dependent on environmental and genetic components. This syndrome affects over 5% of the individuals in Western populations [27]. The pathogenesis of Type 2 diabetes involves abnormalities in both insulin secretion by pancreatic beta cells and peripheral insulin action [28].

The insulin action in target tissues involves a cascade of events initiated by insulin binding to its α subunit of cell surface receptor (IR) [92]. The interaction between insulin and IR results in conformational changes that stimulates the tyrosine autophosphorylation in IR β subunits which result in tyrosine phosphorylation of insulin receptor substrates (IRSs) including IRS1, IRS2 IRS3, IRS4, Gab1, and Shc [18]. Binding of IRSs to the regulatory subunit of phosphoinositide 3-kinase (PI3K) via Src homology 2 (SH2) domains results in activation of PI3K, which phosphorylates membrane phospholipids and phosphatidylinositol 4,5-bisphosphate (PIP2) on the 3' position. This complex activates the 3-phosphoinositide-dependent protein kinases (PDK-1 and PDK-2) resulting in activation of Akt/protein kinase B (PKB) and atypical protein kinase C λ and ζ , (PKC λ/ζ), each of which are serine/threonine kinases which in turn stimulates the glucose transport in the muscle and adipose tissue, glycogen synthesis in the liver and muscle, and lipogenesis in the adipose tissue [17, 19, 92].

Several mechanisms may contribute to the deregulation of the insulin-signaling pathway in metabolic disorders, including reduction in: receptor kinase activity, concentration and phosphorylation of IRS proteins, PIK3 activity and glucose transporters (GLUTs) translocation [21]. Changes in body fat mass and in serum lipids are linked to development of insulin resistance [20, 24, 77]. Here, we investigated the insulin signaling in liver, muscle and adipose tissue of LDLR $^{-/-}$ mice fed a chow or a high-fat diet.

Material and methods

Animals

Animal experiments were approved by the university's Committee for Ethics in Animal Experimentation (CEUA/Unicamp). C57Bl6 wild type (WT) control and LDL receptor deficient mice ($\text{LDLR}^{-/-}$), originally from Jackson Laboratory, Bar Harbor, ME) were obtained locally from colonies maintained at the University Multidisciplinary Center for Biological Research in Laboratory Animals (CEMIB/ Unicamp). The mice were housed at 22 ± 1 °C on a 12 h light/ dark cycle. The mice had access to standard laboratory rodent chow diet (Nuvital CR1, Colombo, Paraná, Brazil) and water ad libitum during 4 months. At the end of this period the mice were distributed in 4 groups: Control (WT), Control hyperlipidic (WTH), Knockout ($\text{LDLR}^{-/-}$) and Knockout hyperlipidic ($\text{LDLR}^{-/-}\text{H}$). WT and $\text{LDLR}^{-/-}$ mice received chow diet and WTH and $\text{LDLR}^{-/-}\text{H}$ were fed a high-fat-diet (Western-type, 40% Kcal by fat) [49] during 30 days (table 1).

Oral glucose tolerance test (oGTT)

Mice were submitted to an oGTT 3 days before the end of experimental period. Mice were fasted for 12 h and a basal blood sample was harvested from the tail tip ($t=0$ min). A glucose load of 1.5 g/kg body weight was then administered by oral gavage and additional blood samples were collected at 15, 30, 60 and 90 min. Glucose levels were measured using a glucose analyzer (Accu-Chek Advantage, Roche Diagnostic®, Switzerland). The area under the curve was calculated for each mouse using the software GraphPadPrism 5.0 .

Plasma biochemical analysis

Mice were anesthetized using ketamine (50 mg/kg, i.p., Parke-Davis, São Paulo, Brazil) and xylazine (16 mg/kg, i.p., Bayer S.A., São Paulo, Brazil) and blood samples were collected from either the retro-orbital plexus or the tail tip. Blood samples were centrifuged at $15.000 \times g$ at 4°C for 15 min. Aliquots of plasma were stored at -80°C until analyses. Total cholesterol (CHOL), triglycerides (TG) and non-esterified fatty acids (NEFA) were measured in fresh plasma in the fasting state (12 h) using standard commercial kits, according to the manufacturer's instructions (Boehringer Mannheim®, Germany; Merck®, Germany and

Wako®, Germany, respectively). Plasma insulin was measured by radioimmunoassay (RIA) using rat insulin standard.

Pancreatic islet isolation and static insulin secretion

The pancreatic islets were isolated from fed mice (20 week-old) by collagenase digestion of pancreases and then selected under a microscope to exclude any contaminating tissues [84]. After isolation, batches of 5 islets from each group were pre-incubated in Krebs-Ringer bicarbonate buffer (KRBB) containing, in mmol/l: 115 NaCl, 5 KCl, 24 NaHCO₃, 2.56 CaCl₂, 1 MgCl₂ and 25 HEPES, pH 7.4 plus 5.6 mmol/l glucose and 0.3% bovine serum albumin (BSA) for 30 min at 37°C. The islets were further incubated for 1 h in KRBB containing 2.8 or 11.1 mmol/l glucose. Aliquots of the supernatant, at the end of the incubation period, were kept at -20°C for posterior insulin measurement by RIA. The total islet insulin content was assessed and no differences between all groups were observed (not shown).

Tissue extraction and immunoprecipitation

Mice were anesthetized with sodium thiopental and used 10–15 min later. As soon as anesthesia was assured by the loss of pedal and corneal reflexes, the abdominal cavity was opened, the portal vein was exposed, and 0.1 ml normal saline with or without insulin (0.6mmol/L) was injected. At 30 sec after the insulin injection, the liver was removed, and 90 sec later, gastrocnemius muscle and adipose tissue were removed, minced coarsely, and homogenized immediately in extraction buffer, as described elsewhere [93]. Extracts were then centrifuged at 15,000 rpm and 4 C for 40 min to remove insoluble material, and the supernatants were used for immunoprecipitation with α -IR β and protein A-Sepharose 6MB (Pharmacia, Uppsala, Sweden).

Protein analysis by immunoblotting

The precipitated proteins and/or whole-tissue extracts were treated with Laemmli sample buffer [94] containing 100 mmol/l dithiothreitol and heated in a boiling water bath for 5 min, after which they were subjected to SDS-PAGE in a Bio-Rad miniature slab gel apparatus (Mini-Protean). For total extracts, 100 μ g of proteins were subjected to SDS-PAGE.

Electrotransfer of proteins from the gel to nitrocellulose was performed for 120 min at 120 V in a Bio-Rad Mini-Protean transfer apparatus [95]. Nonspecific protein binding to the nitrocellulose was reduced by preincubating the filter for 2 h in blocking buffer (5% nonfat dry milk, 10 mm Tris, 150 mm NaCl, 0.02% Tween 20). The nitrocellulose blot was incubated with specific antibodies overnight at 4 C and then incubated with a horseradish peroxidase-conjugated secondary antibody. Immunoreactive bands were revealed using chemiluminescence (SuperSignal West Pico, Pierce) detected using a LAS-3000 CCD camera and quantified with the Aida Analysis software (Fujifilm).

Statistical analysis

Results are presented as means \pm SEM for the number of determinations (n) indicated. The data were analyzed by two-way ANOVA (with Neuman–Keuls post-hoc test). The level of significance was set at $p<0.05$ and analyses were performed using Statistica version 7.0 for Windows (Stat Soft Inc, Tulsa, OK, USA).

Results

Animal features

Body weight was lower whereas the adipose epididymal fat depot was higher in $\text{LDLR}^{-/-}$ compared to WT mice (Table 2). The cumulative food consumption during 30 days was similar in $\text{LDLR}^{-/-}\text{H}$ and WTH, however, the body weight gain was significantly higher in $\text{LDLR}^{-/-}\text{H}$ fed a high-fat-diet ($6,2 \pm 0,4$ vs $4,4 \pm 0,5$) $p<0,05$.

Plasma lipids, glucose, insulin levels

$\text{LDLR}^{-/-}$ mice showed high levels of CHOL, TG and glucose in fasted state compared to WT mice. High-fat-diet increased CHOL and glucose levels in both groups (WTH and $\text{LDLR}^{-/-}\text{H}$). WTH mice showed an increase in fasted plasma insulin levels. The TG levels were increased by high-fat-diet only in $\text{LDLR}^{-/-}\text{H}$. Non-esterified-fatty-acids (NEFA) levels did not differ between groups (Tab. 3).

Oral glucose tolerance test (oGTT)

The increase in blood glucose concentrations induced by an oral glucose load was higher in $\text{LDLR}^{-/-}$ compared to WT mice, as demonstrated previously [52] (Fig. 1A). The high-fat diet worsened the glucose tolerance in these mice ($\text{LDLR}^{-/-}\text{H}$) (Fig. 1A). The incremental area under the curve (AUC) in $\text{LDLR}^{-/-}$ was significantly higher than that of WT mice and high-fat-diet further increased the AUC in these mice (Fig 1. B).

Insulin secretion in isolated islets

Basal insulin secretion (2.8 mmol/l glucose) was similar in all groups of islets. At a stimulatory glucose concentrations (11.1 mmol/l), the insulin secretion was significantly lower in $\text{LDLR}^{-/-}$ compared with WT islets ($p<0.05$). High-fat diet provoked a marginal increase in the insulin secretion in WTH compared with WT islets, whereas the secretion was similar in $\text{LDLR}^{-/-}$ and $\text{LDLR}^{-/-}\text{H}$ islets (Fig. 2).

Insulin signaling in liver, gastrocnemius muscle and epidymal fat tissue

The liver from $\text{LDLR}^{-/-}$ mice showed a significant increase in insulin-induced IR tyrosin and AKT serine phosphorylation compared with WT mice. High-fat-diet significantly reduced insulin-induced IR tyrosin and AKT serine phosphorylation in $\text{LDLR}^{-/-}\text{H}$, ($p<0.05$). No differences between insulin-stimulated IR tyrosin and AKT serine phosphorylation were observed in WTH, compared to WT mice (Fig. 3A and 3B).

In muscle, insulin-induced IR tyrosin and AKT serine phosphorylation were significantly higher in $\text{LDLR}^{-/-}$ than WT mice. Insulin-stimulated IR tyrosin phosphorylation was decreased in both WTH and $\text{LDLR}^{-/-}\text{H}$, however only $\text{LDLR}^{-/-}\text{H}$ showed a tendency to reduce AKT serine phosphorylation (27%), compared with $\text{LDLR}^{-/-}$ (Fig. 4A and 4B).

Finally, in adipose tissue there were no differences in insulin-induced IR tyrosin and AKT serine phosphorylation in $\text{LDLR}^{-/-}$ and WT mice (Fig. 5A and 5B). However, IR tyrosin phosphorylation in basal conditions (vehicle) was higher in $\text{LDLR}^{-/-}$ compared with all the other groups (Fig. 5A). Insulin-induced IR tyrosin and AKT Serine phosphorylation was significantly decreased in $\text{LDLR}^{-/-}\text{H}$ compared with $\text{LDLR}^{-/-}$ ($p<0.05$). No differences in insulin-stimulated IR tyrosin and AKT serine phosphorylation was observed in WTH compared with WT mice (Fig. 5A-5B).

Insulin-degrading-enzyme (IDE) protein expression in liver

We also investigated the protein expression of the IDE in liver of all groups of mice. LDLR^{-/-} showed lower expression of IDE in liver compared with WT mice ($P<0.05$). The high-fat diet promoted a significant reduction in IDE content in both WTH e LDLR^{-/-H} (Fig. 6).

Discussion

Our results showed that LDLR^{-/-} mice, fed a chow diet, exhibit higher epydidimal-fat depot, glucose intolerance, and lower insulin secretion, compared to WT mice (Fig. 1, Tables 1-2). Since higher mass of adipose tissue impairs the insulin signaling in rodents and humans peripheral tissues [22, 76], we analyzed the insulin signaling in liver, gastrocnemius muscle and adipose tissue in these mice. Contrary to what was expected, LDLR^{-/-} showed higher insulin sensitivity, represented by higher IR tyrosine and AKT serine phosphorylation especially in muscle and liver compared with WT mice. In adipose tissue, where the fat depot was significantly increased, IR tyrosine and AKT serine phosphorylation were only marginally increased, after insulin stimulus. However, at basal condition (absence of insulin stimulus), a higher IR tyrosin phosphorylation compared with WT, was observed in LDLR^{-/-} mice. Since in adipose tissue insulin stimulates lipogenesis it is conceivable that the higher IR tyrosin phosphorylation may explain the higher epydidimal fat pad mass in LDLR^{-/-} mice.

It is well accepted that glucose homeostasis depends on adequate insulin secretion by pancreatic beta-cells and action of this hormone in target tissues [19, 75]. As example of this orchestration, it is known that under physical training there is an increase in insulin sensitivity with a concomitant and adaptive reduction in insulin secretion [96]. Also, malnourished mice that secrete less insulin in response to fuel secretagogues have their peripheral tissues more sensitive to the insulin [97, 98]. Thus, the increase in insulin signaling observed in muscle and liver, associated with low IDE expression in LDLR^{-/-} mice, can be an adaptation to the lower insulin secretion observed in these mice. An inverse relationship between IDE activity and cholesterol content was recently proposed based on the observation that lovastatin (cholesterol synthesis inhibitor) increases the degradation of amyloid depots by activation of IDE in microglia cells [99]. Since LDLR^{-/-} mice showed increased cholesterol synthesis in various

tissues, this could be linked to a lower expression of IDE in these mice. However, this hypothesis needs to be confirmed.

High-fat fed $\text{LDLR}^{-/-}$ H mice present a marked deterioration in the lipid plasma profile, as well as in the glucose tolerance. The use of HFD induced an increase in fat depot and marked attenuation in the insulin signaling in liver, muscle and adipose tissue in those mice. It is recognized that a higher fat depots is related to increased insulin resistance mainly because of the action of pro-inflammatory adipokines [100-102]. Also, insulin resistance induced by obesity may be due to the sequential activation of both protein kinase C (PKC) and kinase inhibitor of nuclear factor kB (IKkB) [103, 104]. In addition, in obesity the action of insulin is also attenuated by protein tyrosine phosphatases, for example, PTP1B, which catalyze the rapid dephosphorylation of the insulin receptor and their substrates [105].

In WTH mice the effects of high fat diet on insulin signaling was very mild than in $\text{LDLR}^{-/-}$. In the former mice, HFD reduced only the $\text{IR}\beta$ phosphorylation in muscle. Prada et al [77] demonstrated that rats fed a western type diet showed increase in insulin resistance in a tissue-specific manner that occurred first in muscle and hypothalamus, and later in the liver. However, these authors noticed that hyperinsulinemia was observed only after the increase in insulin resistance in the liver. On the contrary, in our WTH mice, hyperinsulinemia is already present before the onset of insulin resistance in the liver. In $\text{LDLR}^{-/-}$ H mice, although there is insulin resistance in liver, these mice are unable to secrete more insulin in response to fuel secretagogues, thus a more marked hyperglycemia occurs in these mice. The hampered insulin secretion in the islets of these mice is probably due to alterations in calcium handling, as a consequence of the excess of cholesterol in these islets (data not published).

In conclusion, our results indicate that $\text{LDLR}^{-/-}$ mice fed a chow diet are more sensitive to insulin probably due to adaptive mechanisms that compensate lower insulin secretion. However, these changes are not sufficient to maintain glucose homeostasis since these mice were glucose intolerants. However, when fed a high-fat diet, they became also insulin resistant probably due increase adipokine levels as a consequence of increase in visceral adipose tissue mass.

References

- [1] Wild S, Roglic G, Green A, Sicree R, King H (2004) Global prevalence of diabetes: estimates for the year 2000 and projections for 2030. *Diabetes Care* 27: 1047-1053.
- [2] Muoio DM, Newgard CB (2008) Mechanisms of disease: molecular and metabolic mechanisms of insulin resistance and beta-cell failure in type 2 diabetes. *Nat Rev Mol Cell Biol* 9: 193-205.
- [3] White MF, Kahn CR (1994) The insulin signaling system. *J Biol Chem* 269: 1-4.
- [4] Youngren JF (2007) Regulation of insulin receptor function. *Cell Mol Life Sci* 64: 873-891.
- [5] Patti ME, Kahn CR (1998) The insulin receptor--a critical link in glucose homeostasis and insulin action. *J Basic Clin Physiol Pharmacol* 9: 89-109.
- [6] Whiteman EL, Cho H, Birnbaum MJ (2002) Role of Akt/protein kinase B in metabolism. *Trends Endocrinol Metab* 13: 444-451.
- [7] Pessin JE, Saltiel AR (2000) Signaling pathways in insulin action: molecular targets of insulin resistance. *J Clin Invest* 106: 165-169.
- [8] Bergman RN, Ader M (2000) Free fatty acids and pathogenesis of type 2 diabetes mellitus. *Trends Endocrinol Metab* 11: 351-356.
- [9] Shulman GI (2000) Cellular mechanisms of insulin resistance. *J Clin Invest* 106: 171-176.
- [10] Prada PO, Zecchin HG, Gasparetti AL, et al. (2005) Western diet modulates insulin signaling, c-Jun N-terminal kinase activity, and insulin receptor substrate-1ser307 phosphorylation in a tissue-specific fashion. *Endocrinology* 146: 1576-1587.
- [11] Merat S, Casanada F, Sutphin M, Palinski W, Reaven PD (1999) Western-type diets induce insulin resistance and hyperinsulinemia in LDL receptor-deficient mice but do not increase aortic atherosclerosis compared with normoinsulinemic mice in which similar plasma cholesterol levels are achieved by a fructose-rich diet. *Arterioscler Thromb Vasc Biol* 19: 1223-1230.
- [12] Boschero AC, Delattre E (1985) The mechanism of gentamicin-inhibited insulin release by isolated islets. *Arch Int Pharmacodyn Ther* 273: 167-176.
- [13] Torsoni MA, Carvalheira JB, Pereira-Da-Silva M, de Carvalho-Filho MA, Saad MJ, Velloso LA (2003) Molecular and functional resistance to insulin in hypothalamus of rats exposed to cold. *Am J Physiol Endocrinol Metab* 285: E216-223.

- [14] Laemmli UK (1970) Cleavage of structural proteins during the assembly of the head of bacteriophage T4. *Nature* 227: 680-685.
- [15] Towbin H, Staehelin T, Gordon J (1979) Electrophoretic transfer of proteins from polyacrylamide gels to nitrocellulose sheets: procedure and some applications. *Proc Natl Acad Sci U S A* 76: 4350-4354.
- [16] Bonfleur ML, Vanzela EC, Ribeiro RA, et al. (2010) Primary hypercholesterolaemia impairs glucose homeostasis and insulin secretion in low-density lipoprotein receptor knockout mice independently of high-fat diet and obesity. *Biochim Biophys Acta* 1801: 183-190.
- [17] Colditz GA, Willett WC, Rotnitzky A, Manson JE (1995) Weight gain as a risk factor for clinical diabetes mellitus in women. *Ann Intern Med* 122: 481-486.
- [18] Hotamisligil GS, Peraldi P, Budavari A, Ellis R, White MF, Spiegelman BM (1996) IRS-1-mediated inhibition of insulin receptor tyrosine kinase activity in TNF-alpha- and obesity-induced insulin resistance. *Science* 271: 665-668.
- [19] Moller DE, Chang PY, Yaspelkis BB, Flier JS, Wallberg-Henriksson H, Ivy JL (1996) Transgenic mice with muscle-specific insulin resistance develop increased adiposity, impaired glucose tolerance, and dyslipidemia. *Endocrinology* 137: 2397-2405.
- [20] Calegari VC, Zoppi CC, Rezende LF, Silveira LR, Carneiro EM, Boschero AC (2011) Endurance training activates AMP-activated protein kinase, increases expression of uncoupling protein 2 and reduces insulin secretion from rat pancreatic islets. *J Endocrinol* 208: 257-264.
- [21] Reis MA, Carneiro EM, Mello MA, Boschero AC, Saad MJ, Velloso LA (1997) Glucose-induced insulin secretion is impaired and insulin-induced phosphorylation of the insulin receptor and insulin receptor substrate-1 are increased in protein-deficient rats. *J Nutr* 127: 403-410.
- [22] Latorraca MQ, Carneiro EM, Boschero AC, Mello MA (1998) Protein deficiency during pregnancy and lactation impairs glucose-induced insulin secretion but increases the sensitivity to insulin in weaned rats. *Br J Nutr* 80: 291-297.
- [23] Tamboli IY, Barth E, Christian L, et al. (2010) Statins promote the degradation of extracellular amyloid β -peptide by microglia via stimulation of exosome-associated insulin-degrading enzyme (IDE) secretion. *J Biol Chem* 285: 37405-37414.
- [24] McPherson R, Jones PH (2003) The metabolic syndrome and type 2 diabetes: role of the adipocyte. *Curr Opin Lipidol* 14: 549-553.
- [25] Tuomilehto J, Lindström J, Eriksson JG, et al. (2001) Prevention of type 2 diabetes mellitus by changes in lifestyle among subjects with impaired glucose tolerance. *N Engl J Med* 344: 1343-1350.

- [26] Waki H, Tontonoz P (2007) Endocrine functions of adipose tissue. *Annu Rev Pathol* 2: 31-56.
- [27] Shoelson SE, Lee J, Yuan M (2003) Inflammation and the IKK beta/I kappa B/NF-kappa B axis in obesity- and diet-induced insulin resistance. *Int J Obes Relat Metab Disord* 27 Suppl 3: S49-52.
- [28] De Fea K, Roth RA (1997) Protein kinase C modulation of insulin receptor substrate-1 tyrosine phosphorylation requires serine 612. *Biochemistry* 36: 12939-12947.
- [29] Elchebly M, Payette P, Michaliszyn E, et al. (1999) Increased insulin sensitivity and obesity resistance in mice lacking the protein tyrosine phosphatase-1B gene. *Science* 283: 1544-1548.

TABLES

Table 1 – Composition of high-fat diet.

Components	g/Kg
Casein	195.0
Cornstarch	320.7
Dextrinized cornstarch	79.6
Lard	50.0
Butter	204.0
Cellulose	50.0
Mineral mix AIN-93M	35.0
Vitamin mix AIN-93M	10.0
L-Cystine	1.8
Choline bitartrate	2.5
Sucrose	51.4

Table 2. Body weight, epididymal and retroperitoneal fat depot in mice fed with chow diet (WT e LDLR^{-/-}) and high-fat diet (WTH e LDLR^{-/-H}).

Group	Body weight (g)	Epididymal fat	Retroperitoneal fat	n
		(% body weight)	(% body weight)	
WT	28,0 ± 0,8	0,8 ± 0,1	0,5 ± 0,03	14
WTH	32,7 ± 1,0*	3,1 ± 0,3*	1,5 ± 0,14*	11
LDLR ^{-/-}	25,3 ± 0,7*	1,2 ± 0,1*	0,6 ± 0,09	16
LDLR ^{-/-H}	30,9 ± 0,8**#	4,0 ± 0,2**#¥	1,8 ± 0,21**#	16

Values are means ± SEM; n (mice number). * p<0,05 vs WT; # p<0,05 vs LDLR^{-/-}; ¥ vs WTH.

Table 3. Glucose, insulin and plasma lipids in mice fed with chow diet (WT e LDLR^{-/-}) and high-fat diet (WTH e LDLR^{-/-H}).

Parameters		Group				n
		WT	WTH	LDLR ^{-/-}	LDLR ^{-/-H}	
Glucose (mg/dL)	Fasted	75 ± 3,2	88,0± 3,4 [*]	86,4±2,6 [*]	106,6+4,4 ^{*#}	14-17
	Fed	118,7±4,9	142,9±5,4 [*]	142,3±6,7 [*]	161,1±7,5 ^{*#}	12-15
Insulin (pg/mL)	Fasted	133,0±5,7	194,8±7,1 [*]	95,4±1,3 [*]	101,8±3,5 [*]	6-7
	Fasted	108,1±5,6	170,6±7,5 [*]	294,3±11,6 [*]	906,0±35,0 ^{*#}	13-16
Cholesterol (mg/dL)	Fasted	56,9±2,9	70,8±2,9	127,7±7,8 [*]	201,5±9,7 ^{*#}	12-18
	Fasted	0,81±0,09	1,00±0,12	0,79±0,04	1,06±0,05	8
Triglycerides (mg/dL)						
NEFA (mmol/L)						

Values are means ± SEM; n (mice number). * p<0.05 vs WT; # p<0.05 vs LDLR^{-/-}.

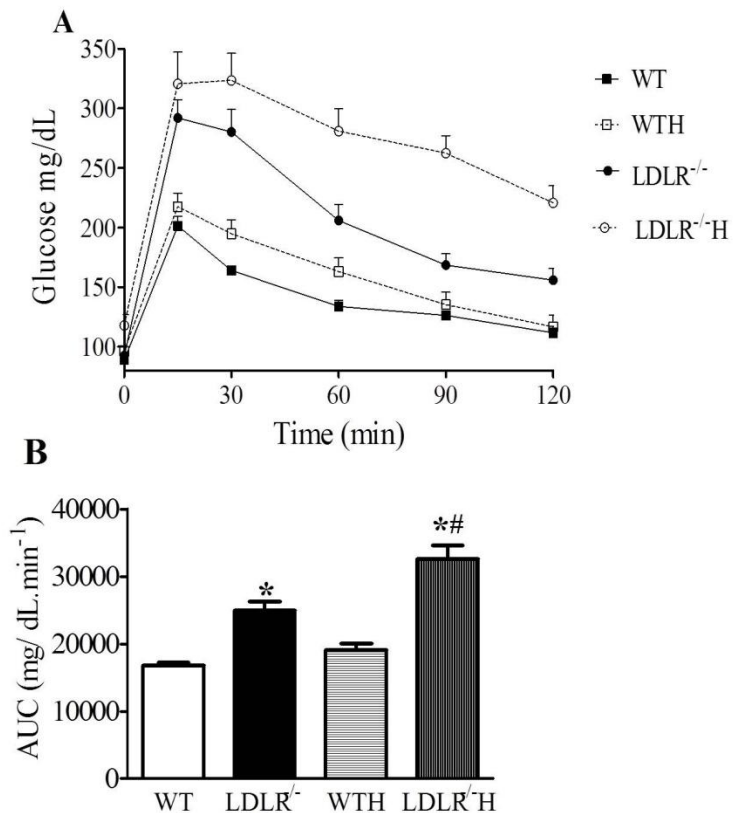
FIGURES

Figure 1. (A) – Blood glucose during a glucose tolerance test (oGTT) in WT (solid squares), WTH (open squares), LDLR^{-/-} (solid circles) e LDLR^{-/-}H (open circles). (B) - Area under the curve (AUC) during the oGTT test. The bars represent means \pm SEM of the AUC of each mice, n=8-10. * p<0.05 compared WT; # p<0.05 compared LDLR^{-/-}.

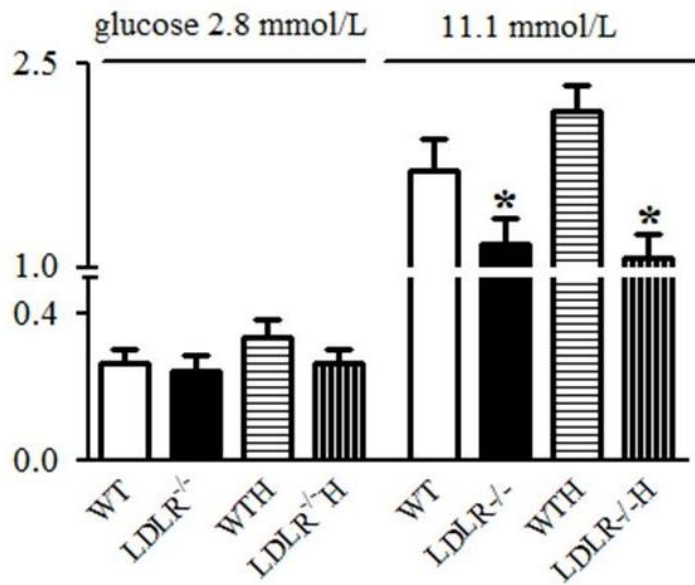


Figure 2. Insulin secretion stimulated by 2.8mmol/L and 11.1 mmol/L of glucose. Bars represent means \pm SEM of the 12-20 groups of islets of 6 different mice. * vs WT $p < 0.05$.

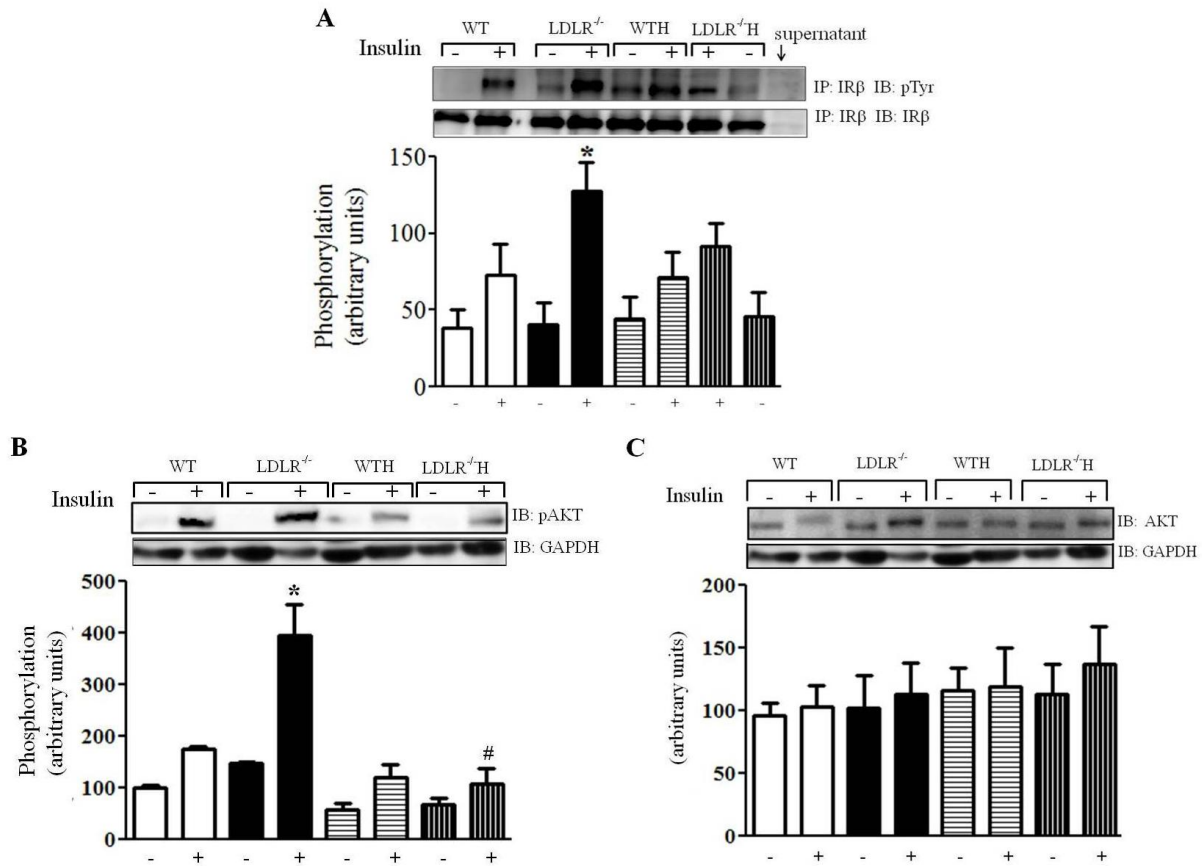


Figure 3. Insulin signaling in liver of mice fed chow diet (WT e LDLR^{-/-}) and high-fat-diet (WTH e LDLR^{-/-H}). A. Imunoprecipitation (IP) with α -IR β (IR β) and imunoblotting (IB) with α -phosphorylated-tyrosine (pTyr) or α -IR β antibodies. B. Imunoblotting with α -phosphorylated-AKT (pAKT). C. Imunoblotting with α -AKT1/2/3 (AKT). The bars represent means \pm SEM of the values determined by optical densitometry. n = (4-5). * p<0.05 compared WT stimulated with exogenous insulin; # p<0.05 compared LDLR^{-/-} stimulated with exogenous insulin.

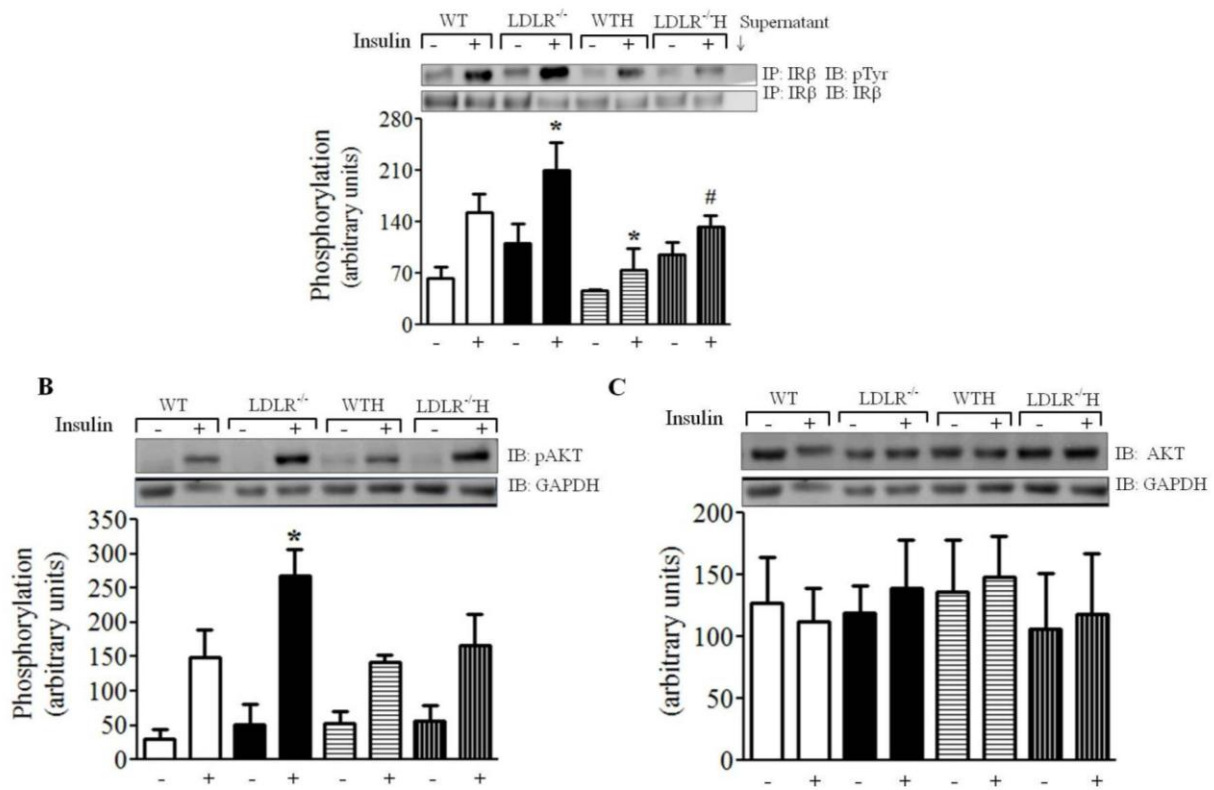


Figure 4. Insulin signaling in gastrocnemius muscle of mice fed chow diet (WT e $\text{LDLR}^{-/-}$) and high-fat diet (WTH e $\text{LDLR}^{-/-}\text{H}$). A. Imunoprecipitation (IP) with α -IR β (IR β) and imunoblotting (IB) with α -phosphorylated-tyrosine (pTyr) or α -IR β antibodies. B. Imunoblotting with α -phosphorylated-AKT (pAKT). C. Imunoblotting with α -AKT1/2/3 (AKT). The bars represent means \pm SEM of the values determined by optical densitometry. n = (3-5). * p<0.05 compared WT stimulated with exogenous insulin; # p<0.05 compared $\text{LDLR}^{-/-}$ stimulated with exogenous insulin.

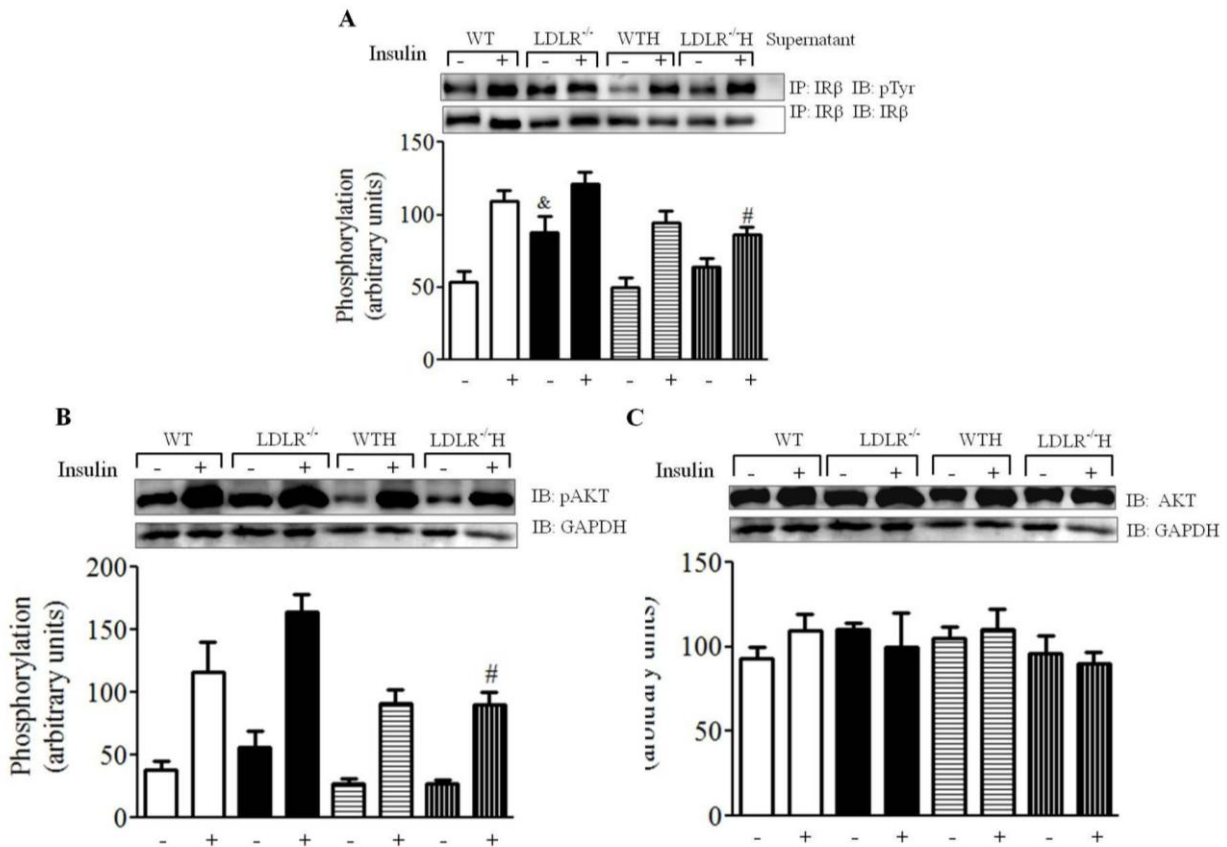


Figure 5. Insulin signaling in adipose tissue of mice fed chow diet (WT e $LDLR^{-/-}$) and high-fat-diet (WTH e $LDLR^{-/-}H$). A. Imunoprecipitation (IP) with α -IR β (IR β) and imunoblotting (IB) with α -phosphorylated-tyrosine (pTyr) or α -IR β antibodies. B. Imunoblotting with α -phosphorylated-AKT (pAKT). C. Imunoblotting with α -AKT1/2/3 (AKT). The bars represent means \pm SEM of the values determined by optical densitometry. n = (4-5). & p<0.05 compared WT without exogenous insulin stimulus; # p<0.05 compared $LDLR^{-/-}$ stimulated with exogenous insulin.

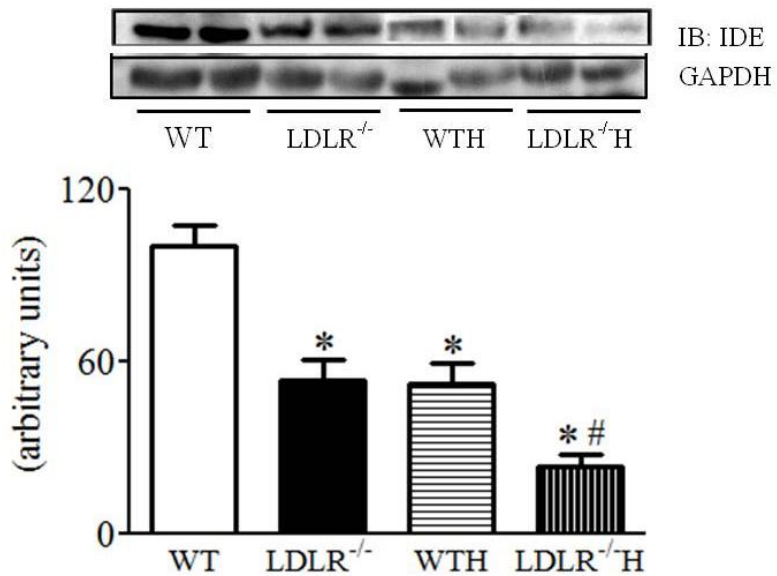


Figure 6. Insulin-degrading-enzyme (IDE) protein expression in liver from WT (open bars) and $\text{LDLR}^{-/-}$ (dark bars), WTH (bars with horizontal lines) and $\text{LDLR}^{-/-}\text{H}$ (bars with vertical lines) mice. Protein extracts were processed for Western blotting. The bars represent means \pm SEM of the values determined by optical densitometry. n = (5). * $p<0.05$ compared WT; # $p<0.05$ compared $\text{LDLR}^{-/-}$.

CONCLUSÃO GERAL

A análise conjunta dos resultados nos permitiu concluir que:

- Tanto o aumento quanto a diminuição excessiva do conteúdo de colesterol nas ilhotas alteram a movimentação de cálcio e consequentemente a secreção de insulina. A redução do colesterol nas ilhotas dos $LDLR^{-/-}$ reverteu estas alterações.
- Camundongos $LDLR^{-/-}$, alimentados com dieta padrão, são mais sensíveis à insulina, provavelmente como um mecanismo adaptativo a menor secreção deste hormônio. No entanto, estas adaptações não são suficientes para manter a homeostase glicêmica visto que estes animais são intolerantes à glicose.
- Quando alimentados com dieta hiperlipídica camundongos $LDLR^{-/-}$ se tornam resistentes a insulina. O desenvolvimento da resistência nestes camundongos se deve, provavelmente, ao aumento do tecido adiposo visceral provocado pela dieta hiperlipídica.

REFERÊNCIAS BIBLIOGRÁFICAS

- [1] Boschero AC (1996) Acoplamento da estimulação-secreção de insulina pelas células beta pancreáticas. *Arq Bras Endocrinol Metab* 40: 7
- [2] Thorens B, Sarkar HK, Kaback HR, Lodish HF (1988) Cloning and functional expression in bacteria of a novel glucose transporter present in liver, intestine, kidney, and beta-pancreatic islet cells. *Cell* 55: 281-290
- [3] Malaisse WJ, Carpinelli AR, Sener A (1981) Stimulus-secretion coupling of glucose-induced insulin release. Timing of early metabolic, ionic, and secretory events. *Metabolism* 30: 527-532
- [4] Prentki M, Matschinsky FM (1987) Ca²⁺, cAMP, and phospholipid-derived messengers in coupling mechanisms of insulin secretion. *Physiol Rev* 67: 1185-1248
- [5] Delmeire D, Flamez D, Hinke SA, Cali JJ, Pipeleers D, Schuit F (2003) Type VIII adenylyl cyclase in rat beta cells: coincidence signal detector/generator for glucose and GLP-1. *Diabetologia* 46: 1383-1393
- [6] Dyachok O, Idevall-Hagren O, Sågertorp J, et al. (2008) Glucose-induced cyclic AMP oscillations regulate pulsatile insulin secretion. *Cell Metab* 8: 26-37
- [7] Rutter GA (2001) Nutrient-secretion coupling in the pancreatic islet beta-cell: recent advances. *Mol Aspects Med* 22: 247-284
- [8] Eliasson L, Abdulkader F, Braun M, Galvanovskis J, Hoppa MB, Rorsman P (2008) Novel aspects of the molecular mechanisms controlling insulin secretion. *J Physiol* 586: 3313-3324
- [9] Newsholme P, Bender K, Kiely A, Brennan L (2007) Amino acid metabolism, insulin secretion and diabetes. *Biochem Soc Trans* 35: 1180-1186
- [10] Dura E, Jijakli H, Zhang HX, Oguzhan B, Sener A, Malaisse WJ (2002) Insulinotropic action of amino acids at their physiological concentrations: I. Experiments in incubated islets. *Int J Mol Med* 9: 527-531
- [11] McClenaghan NH (2007) Physiological regulation of the pancreatic {beta}-cell: functional insights for understanding and therapy of diabetes. *Exp Physiol* 92: 481-496
- [12] Gilon P, Henquin JC (2001) Mechanisms and physiological significance of the cholinergic control of pancreatic beta-cell function. *Endocr Rev* 22: 565-604
- [13] Boschero AC, Szpak-Glasman M, Carneiro EM, et al. (1995) Oxotremorine-m potentiation of glucose-induced insulin release from rat islets involves M3 muscarinic receptors. *Am J Physiol* 268: E336-342

- [14] White MF (1997) The insulin signalling system and the IRS proteins. *Diabetologia* 40 Suppl 2: S2-17
- [15] JBC C, HG Z, MJA S (2002) Vias de Sinalização da Insulina. *Arq Bras Endocrinol Metab* 46: 7
- [16] Kasuga M, Zick Y, Blith DL, Karlsson FA, Häring HU, Kahn CR (1982) Insulin stimulation of phosphorylation of the beta subunit of the insulin receptor. Formation of both phosphoserine and phosphotyrosine. *J Biol Chem* 257: 9891-9894
- [17] Whiteman EL, Cho H, Birnbaum MJ (2002) Role of Akt/protein kinase B in metabolism. *Trends Endocrinol Metab* 13: 444-451
- [18] Youngren JF (2007) Regulation of insulin receptor function. *Cell Mol Life Sci* 64: 873-891
- [19] Patti ME, Kahn CR (1998) The insulin receptor--a critical link in glucose homeostasis and insulin action. *J Basic Clin Physiol Pharmacol* 9: 89-109
- [20] Shulman GI (2000) Cellular mechanisms of insulin resistance. *J Clin Invest* 106: 171-176
- [21] Pessin JE, Saltiel AR (2000) Signaling pathways in insulin action: molecular targets of insulin resistance. *J Clin Invest* 106: 165-169
- [22] Colditz GA, Willett WC, Rotnitzky A, Manson JE (1995) Weight gain as a risk factor for clinical diabetes mellitus in women. *Ann Intern Med* 122: 481-486
- [23] Kahn BB, Flier JS (2000) Obesity and insulin resistance. *J Clin Invest* 106: 473-481
- [24] Bergman RN, Ader M (2000) Free fatty acids and pathogenesis of type 2 diabetes mellitus. *Trends Endocrinol Metab* 11: 351-356
- [25] Guyton A, Hall J (2006) Textbook of medical physiology, Filadelfia
- [26] (1997) Report of the Expert Committee on the Diagnosis and Classification of Diabetes Mellitus. *Diabetes Care* 20: 1183-1197
- [27] Wild S, Roglic G, Green A, Sicree R, King H (2004) Global prevalence of diabetes: estimates for the year 2000 and projections for 2030. *Diabetes Care* 27: 1047-1053
- [28] Muoio DM, Newgard CB (2008) Mechanisms of disease: molecular and metabolic mechanisms of insulin resistance and beta-cell failure in type 2 diabetes. *Nat Rev Mol Cell Biol* 9: 193-205
- [29] Sacks DB, McDonald JM (1996) The pathogenesis of type II diabetes mellitus. A polygenic disease. *Am J Clin Pathol* 105: 149-156

- [30] Adiels M, Olofsson SO, Taskinen MR, Borén J (2006) Diabetic dyslipidaemia. *Curr Opin Lipidol* 17: 238-246
- [31] Ginsberg HN (1996) Diabetic dyslipidemia: basic mechanisms underlying the common hypertriglyceridemia and low HDL cholesterol levels. *Diabetes* 45 Suppl 3: S27-30
- [32] Wilson PW, McGee DL, Kannel WB (1981) Obesity, very low density lipoproteins, and glucose intolerance over fourteen years: The Framingham Study. *Am J Epidemiol* 114: 697-704
- [33] Lewis GF, Carpentier A, Adeli K, Giacca A (2002) Disordered fat storage and mobilization in the pathogenesis of insulin resistance and type 2 diabetes. *Endocr Rev* 23: 201-229
- [34] Reaven GM, Chen YD, Jeppesen J, Maheux P, Krauss RM (1993) Insulin resistance and hyperinsulinemia in individuals with small, dense low density lipoprotein particles. *J Clin Invest* 92: 141-146
- [35] von Eckardstein A, Schulte H, Assmann G (2000) Risk for diabetes mellitus in middle-aged Caucasian male participants of the PROCAM study: implications for the definition of impaired fasting glucose by the American Diabetes Association. *Prospective Cardiovascular Münster. J Clin Endocrinol Metab* 85: 3101-3108
- [36] Dunn FL (2010) Management of dyslipidemia in people with type 2 diabetes mellitus. *Rev Endocr Metab Disord* 11: 41-51
- [37] Cnop M, Hannaert JC, Grupping AY, Pipeleers DG (2002) Low density lipoprotein can cause death of islet beta-cells by its cellular uptake and oxidative modification. *Endocrinology* 143: 3449-3453
- [38] Roehrich ME, Mooser V, Lenain V, et al. (2003) Insulin-secreting beta-cell dysfunction induced by human lipoproteins. *J Biol Chem* 278: 18368-18375
- [39] Rütti S, Ehses JA, Sibler RA, et al. (2009) Low- and high-density lipoproteins modulate function, apoptosis, and proliferation of primary human and murine pancreatic beta-cells. *Endocrinology* 150: 4521-4530
- [40] Abderrahmani A, Niederhauser G, Favre D, et al. (2007) Human high-density lipoprotein particles prevent activation of the JNK pathway induced by human oxidised low-density lipoprotein particles in pancreatic beta cells. *Diabetologia* 50: 1304-1314
- [41] Pétremand J, Bulat N, Butty AC, et al. (2009) Involvement of 4E-BP1 in the protection induced by HDLs on pancreatic beta-cells. *Mol Endocrinol* 23: 1572-1586
- [42] Paigen B, Plump AS, Rubin EM (1994) The mouse as a model for human cardiovascular disease and hyperlipidemia. *Curr Opin Lipidol* 5: 258-264

- [43] Breslow JL (1996) Mouse models of atherosclerosis. *Science* 272: 685-688
- [44] Ishibashi S, Brown MS, Goldstein JL, Gerard RD, Hammer RE, Herz J (1993) Hypercholesterolemia in low density lipoprotein receptor knockout mice and its reversal by adenovirus-mediated gene delivery. *J Clin Invest* 92: 883-893
- [45] Pauciullo P, Mancini M (1998) Treatment challenges in hypercholesterolemia. *Cardiovasc Drugs Ther* 12: 325-337
- [46] Ishibashi S, Goldstein JL, Brown MS, Herz J, Burns DK (1994) Massive xanthomatosis and atherosclerosis in cholesterol-fed low density lipoprotein receptor-negative mice. *J Clin Invest* 93: 1885-1893
- [47] Schreyer SA, Vick C, Lystig TC, Mystkowski P, LeBoeuf RC (2002) LDL receptor but not apolipoprotein E deficiency increases diet-induced obesity and diabetes in mice. *Am J Physiol Endocrinol Metab* 282: E207-214
- [48] Li AC, Brown KK, Silvestre MJ, Willson TM, Palinski W, Glass CK (2000) Peroxisome proliferator-activated receptor gamma ligands inhibit development of atherosclerosis in LDL receptor-deficient mice. *J Clin Invest* 106: 523-531
- [49] Merat S, Casanada F, Sutphin M, Palinski W, Reaven PD (1999) Western-type diets induce insulin resistance and hyperinsulinemia in LDL receptor-deficient mice but do not increase aortic atherosclerosis compared with normoinsulinemic mice in which similar plasma cholesterol levels are achieved by a fructose-rich diet. *Arterioscler Thromb Vasc Biol* 19: 1223-1230
- [50] Kowaltowski AJ, Castilho RF, Vercesi AE (2001) Mitochondrial permeability transition and oxidative stress. *FEBS Lett* 495: 12-15
- [51] Oliveira HC, Cocco RG, Alberici LC, et al. (2005) Oxidative stress in atherosclerosis-prone mouse is due to low antioxidant capacity of mitochondria. *FASEB J* 19: 278-280
- [52] Bonfleur ML, Vanzela EC, Ribeiro RA, et al. (2010) Primary hypercholesterolaemia impairs glucose homeostasis and insulin secretion in low-density lipoprotein receptor knockout mice independently of high-fat diet and obesity. *Biochim Biophys Acta* 1801: 183-190
- [53] Quintão E, Nakandakare E, Passarelli M (2011) Lípidos: do metabolismo à aterosclerose. São Paulo
- [54] Chang TY, Chang CC, Ohgami N, Yamauchi Y (2006) Cholesterol sensing, trafficking, and esterification. *Annu Rev Cell Dev Biol* 22: 129-157
- [55] Yvan-Charvet L, Wang N, Tall AR (2010) Role of HDL, ABCA1, and ABCG1 transporters in cholesterol efflux and immune responses. *Arterioscler Thromb Vasc Biol* 30: 139-143

- [56] Lehninger AL, Nelson DL, Cox MM (2006) Principios de Bioquímica. Sarvier, São Paulo
- [57] Brown MS, Goldstein JL (1986) A receptor-mediated pathway for cholesterol homeostasis. *Science* 232: 34-47
- [58] Brown MS, Goldstein JL (1997) The SREBP pathway: regulation of cholesterol metabolism by proteolysis of a membrane-bound transcription factor. *Cell* 89: 331-340
- [59] Ikonen E (2008) Cellular cholesterol trafficking and compartmentalization. *Nat Rev Mol Cell Biol* 9: 125-138
- [60] Hozoji M, Munehira Y, Ikeda Y, et al. (2008) Direct interaction of nuclear liver X receptor-beta with ABCA1 modulates cholesterol efflux. *J Biol Chem* 283: 30057-30063
- [61] Ohvo-Rekilä H, Ramstedt B, Leppimäki P, Slotte JP (2002) Cholesterol interactions with phospholipids in membranes. *Prog Lipid Res* 41: 66-97
- [62] Róg T, Pasenkiewicz-Gierula M (2003) Effects of epicholesterol on the phosphatidylcholine bilayer: a molecular simulation study. *Biophys J* 84: 1818-1826
- [63] Brown DA, London E (1998) Structure and origin of ordered lipid domains in biological membranes. *J Membr Biol* 164: 103-114
- [64] Churchward MA, Rogasevskaya T, Höfgen J, Bau J, Coorssen JR (2005) Cholesterol facilitates the native mechanism of Ca²⁺-triggered membrane fusion. *J Cell Sci* 118: 4833-4848
- [65] Wiser O, Trus M, Hernández A, et al. (1999) The voltage sensitive Lc-type Ca²⁺ channel is functionally coupled to the exocytotic machinery. *Proc Natl Acad Sci U S A* 96: 248-253
- [66] Xia F, Gao X, Kwan E, et al. (2004) Disruption of pancreatic beta-cell lipid rafts modifies Kv2.1 channel gating and insulin exocytosis. *J Biol Chem* 279: 24685-24691
- [67] Lang T, Bruns D, Wenzel D, et al. (2001) SNAREs are concentrated in cholesterol-dependent clusters that define docking and fusion sites for exocytosis. *EMBO J* 20: 2202-2213
- [68] Ohara-Imaizumi M, Nishiwaki C, Nakamichi Y, Kikuta T, Nagai S, Nagamatsu S (2004) Correlation of syntaxin-1 and SNAP-25 clusters with docking and fusion of insulin granules analysed by total internal reflection fluorescence microscopy. *Diabetologia* 47: 2200-2207
- [69] Ishikawa M, Iwasaki Y, Yatoh S, et al. (2008) Cholesterol accumulation and diabetes in pancreatic beta-cell-specific SREBP-2 transgenic mice: a new model for lipotoxicity. *J Lipid Res* 49: 2524-2534

- [70] Hao M, Head WS, Gunawardana SC, Hasty AH, Piston DW (2007) Direct effect of cholesterol on insulin secretion: a novel mechanism for pancreatic beta-cell dysfunction. *Diabetes* 56: 2328-2338
- [71] Brunham LR, Kruit JK, Pape TD, et al. (2007) Beta-cell ABCA1 influences insulin secretion, glucose homeostasis and response to thiazolidinedione treatment. *Nat Med* 13: 340-347
- [72] Vergeer M, Brunham LR, Koetsveld J, et al. (2010) Carriers of loss-of-function mutations in ABCA1 display pancreatic beta-cell dysfunction. *Diabetes Care* 33: 869-874
- [73] Xia F, Xie L, Mihic A, et al. (2008) Inhibition of cholesterol biosynthesis impairs insulin secretion and voltage-gated calcium channel function in pancreatic beta-cells. *Endocrinology* 149: 5136-5145
- [74] Vikman J, Jimenez-Feltström J, Nyman P, Thelin J, Eliasson L (2009) Insulin secretion is highly sensitive to desorption of plasma membrane cholesterol. *FASEB J* 23: 58-67
- [75] Moller DE, Chang PY, Yaspelkis BB, Flier JS, Wallberg-Henriksson H, Ivy JL (1996) Transgenic mice with muscle-specific insulin resistance develop increased adiposity, impaired glucose tolerance, and dyslipidemia. *Endocrinology* 137: 2397-2405
- [76] Hotamisligil GS, Peraldi P, Budavari A, Ellis R, White MF, Spiegelman BM (1996) IRS-1-mediated inhibition of insulin receptor tyrosine kinase activity in TNF-alpha- and obesity-induced insulin resistance. *Science* 271: 665-668
- [77] Prada PO, Zecchin HG, Gasparetti AL, et al. (2005) Western diet modulates insulin signaling, c-Jun N-terminal kinase activity, and insulin receptor substrate-1ser307 phosphorylation in a tissue-specific fashion. *Endocrinology* 146: 1576-1587
- [78] Bonfleur ML, Ribeiro RA, Balbo SL, et al. (2011) Lower expression of PKA α impairs insulin secretion in islets isolated from low-density lipoprotein receptor (LDLR(-/-)) knockout mice. *Metabolism* 60: 1158-1164
- [79] Perley MJ, Kipnis DM (1967) Plasma insulin responses to oral and intravenous glucose: studies in normal and diabetic subjects. *J Clin Invest* 46: 1954-1962
- [80] Cerf ME (2007) High fat diet modulation of glucose sensing in the beta-cell. *Med Sci Monit* 13: RA12-17
- [81] Eto K, Yamashita T, Matsui J, Terauchi Y, Noda M, Kadowaki T (2002) Genetic manipulations of fatty acid metabolism in beta-cells are associated with dysregulated insulin secretion. *Diabetes* 51 Suppl 3: S414-420
- [82] de Souza JC, de Oliveira CA, Carneiro EM, Boschero AC, de Oliveira HC (2010) Cholesterol toxicity in pancreatic islets from LDL receptor-deficient mice. *Diabetologia* 53: 2461-2462; author reply 2463-2464

- [83] Rizzo MA, Magnuson MA, Drain PF, Piston DW (2002) A functional link between glucokinase binding to insulin granules and conformational alterations in response to glucose and insulin. *J Biol Chem* 277: 34168-34175
- [84] Boschero AC, Delattre E (1985) The mechanism of gentamicin-inhibited insulin release by isolated islets. *Arch Int Pharmacodyn Ther* 273: 167-176
- [85] Scott AM, Atwater I, Rojas E (1981) A method for the simultaneous measurement of insulin release and B cell membrane potential in single mouse islets of Langerhans. *Diabetologia* 21: 470-475
- [86] Bradford MM (1976) A rapid and sensitive method for the quantitation of microgram quantities of protein utilizing the principle of protein-dye binding. *Anal Biochem* 72: 248-254
- [87] Colell A, García-Ruiz C, Lluis JM, Coll O, Mari M, Fernández-Checa JC (2003) Cholesterol impairs the adenine nucleotide translocator-mediated mitochondrial permeability transition through altered membrane fluidity. *J Biol Chem* 278: 33928-33935
- [88] Lundbaek JA, Birn P, Girshman J, Hansen AJ, Andersen OS (1996) Membrane stiffness and channel function. *Biochemistry* 35: 3825-3830
- [89] Takahashi N, Hatakeyama H, Okado H, et al. (2004) Sequential exocytosis of insulin granules is associated with redistribution of SNAP25. *J Cell Biol* 165: 255-262
- [90] Kruit JK, Kremer PH, Dai L, et al. (2010) Cholesterol efflux via ATP-binding cassette transporter A1 (ABCA1) and cholesterol uptake via the LDL receptor influences cholesterol-induced impairment of beta cell function in mice. *Diabetologia* 53: 1110-1119
- [91] Hao M, Bogan JS (2009) Cholesterol regulates glucose-stimulated insulin secretion through phosphatidylinositol 4,5-bisphosphate. *J Biol Chem* 284: 29489-29498
- [92] White MF, Kahn CR (1994) The insulin signaling system. *J Biol Chem* 269: 1-4
- [93] Torsoni MA, Carvalheira JB, Pereira-Da-Silva M, de Carvalho-Filho MA, Saad MJ, Velloso LA (2003) Molecular and functional resistance to insulin in hypothalamus of rats exposed to cold. *Am J Physiol Endocrinol Metab* 285: E216-223
- [94] Laemmli UK (1970) Cleavage of structural proteins during the assembly of the head of bacteriophage T4. *Nature* 227: 680-685
- [95] Towbin H, Staehelin T, Gordon J (1979) Electrophoretic transfer of proteins from polyacrylamide gels to nitrocellulose sheets: procedure and some applications. *Proc Natl Acad Sci U S A* 76: 4350-4354
- [96] Calegari VC, Zoppi CC, Rezende LF, Silveira LR, Carneiro EM, Boschero AC (2011) Endurance training activates AMP-activated protein kinase, increases expression of

uncoupling protein 2 and reduces insulin secretion from rat pancreatic islets. J Endocrinol 208: 257-264

[97] Reis MA, Carneiro EM, Mello MA, Boschero AC, Saad MJ, Velloso LA (1997) Glucose-induced insulin secretion is impaired and insulin-induced phosphorylation of the insulin receptor and insulin receptor substrate-1 are increased in protein-deficient rats. J Nutr 127: 403-410

[98] Latorraca MQ, Carneiro EM, Boschero AC, Mello MA (1998) Protein deficiency during pregnancy and lactation impairs glucose-induced insulin secretion but increases the sensitivity to insulin in weaned rats. Br J Nutr 80: 291-297

[99] Tamboli IY, Barth E, Christian L, et al. (2010) Statins promote the degradation of extracellular amyloid β -peptide by microglia via stimulation of exosome-associated insulin-degrading enzyme (IDE) secretion. J Biol Chem 285: 37405-37414

[100] McPherson R, Jones PH (2003) The metabolic syndrome and type 2 diabetes: role of the adipocyte. Curr Opin Lipidol 14: 549-553

[101] Tuomilehto J, Lindström J, Eriksson JG, et al. (2001) Prevention of type 2 diabetes mellitus by changes in lifestyle among subjects with impaired glucose tolerance. N Engl J Med 344: 1343-1350

[102] Waki H, Tontonoz P (2007) Endocrine functions of adipose tissue. Annu Rev Pathol 2: 31-56

[103] Shoelson SE, Lee J, Yuan M (2003) Inflammation and the IKK beta/I kappa B/NF-kappa B axis in obesity- and diet-induced insulin resistance. Int J Obes Relat Metab Disord 27 Suppl 3: S49-52

[104] De Fea K, Roth RA (1997) Protein kinase C modulation of insulin receptor substrate-1 tyrosine phosphorylation requires serine 612. Biochemistry 36: 12939-12947

[105] Elchebly M, Payette P, Michaliszyn E, et al. (1999) Increased insulin sensitivity and obesity resistance in mice lacking the protein tyrosine phosphatase-1B gene. Science 283: 1544-1548

ANEXO I

DECLARAÇÃO

Declaro para os devidos fins que o conteúdo da minha tese de Doutorado intitulada Secrecção e ação da insulina em camundongos knockout para o receptor de LDL (LDLR^{-/-}) alimentados com dieta padrão ou hiperlipídica:

() não se enquadra no § 3º do Artigo 1º da Informação CCPG 01/08, referente a bioética e biossegurança.

Tem autorização da(s) seguinte(s) Comissão(ões):

() CIBio – Comissão Interna de Biossegurança , projeto No. _____, Instituição:

() CEUA – Comissão de Ética no Uso de Animais , projeto No.1751-1, Instituição: UNICAMP,

() CEP - Comissão de Ética em Pesquisa, protocolo No. _____, Instituição:

* Caso a Comissão seja externa ao IB/UNICAMP, anexar o comprovante de autorização dada ao trabalho. Se a autorização não tiver vínculo direto com o trabalho da tese ou dissertação, deverá ser anexado também um comprovante do vínculo do trabalho do aluno com o que constar no documento de autorização apresentado.



Alyrio. (nome completo)



Basílio
Orientador. (nome completo)

Para uso da Comissão ou Comitê pertinente:

() Deferido () Indeferido



Profa. Dra. ANA MARIA APARECIDA GUARALDO

Presidente da CEUA/UNICAMP

Para uso da Comissão ou Comitê pertinente:

() Deferido () Indeferido

Carimbo e assinatura

ANEXO II



Of. CIBio/IB 06/2008

Cidade Universitária "Zcfrino Vaz",
26 de maio de 2008.

Prof. Dr. EVERARDO MAGALHÃES CARNEIRO
Chefe do Departamento de Fisiologia e Biofísica
Instituto de Biologia
Unicamp

Prezado Professor:

Informamos que o projeto abaixo relacionado, envolvendo OGM do tipo I, sob responsabilidade da **Profa. Dra. Helena C. F. Oliveira**, protocolado sob o número **2008/02**, foi aprovado pela CIBio/IB/Unicamp em Reunião Ordinária realizada no dia 26 de maio de 2008 e para ser desenvolvido nas dependências do Departamento de Fisiologia e Biofísica do Instituto de Biologia da Unicamp:

No. Projeto (data da aprovação)	Data de recepção	Nome do Projeto	Prazo para envio de relatório à CIBio
CIBio 2008/02 (26/05/2008)	22/04/2008	Repercussão de modificações da expressão de proteínas envolvidas no transporte de lipides sobre o metabolismo de lipides e carboidratos, estresse oxidativo e adiposidade em camundongos geneticamente modificados	Fevereiro de 2009 (ref. período 1/1/2008 a 31/12/2008)

Recomendamos que sejam observadas as instruções normativas referentes a transporte e contenção da OGMs, disponíveis na webpage da CTNBio <www.ctnbio.gov.br>.

Atenciosamente,

Cordiais Saudações,

A handwritten signature in blue ink, appearing to read "Anilian Patti".

Profa. Dra. MARIA SILVIA VICCARI GATTI
CIBio/IB-Unicamp

CÓPIA

Cópias: Profa. Dra. Helena C. F. Oliveira